Transcriptome analysis of pod mutant reveals plant hormones are important regulators in controlling pod size in peanut (*Arachis hypogaea* L.)

Yaqi Wang[1,2], Maoning Zhang[2], Pei Du[2], Hua Liu[2], Zhongxin Zhang[2], Jing Xu[2], Li Qin[2], Bingyan Huang[2], Zheng Zheng[2], Wenzhao Dong[2], Xinyou Zhang[1,2] and Suoyi Han[2]

[1] College of Agronomy, Shenyang Agricultural University, Shenyang, China
[2] Henan Academy of Crop Molecular Breeding, Henan Academy of Agricultural Sciences, Zhengzhou, China

ABSTRACT

Pod size is an important yield-influencing trait in peanuts. It is affected by plant hormones and identifying the genes related to these hormones may contribute to pod-related trait improvements in peanut breeding programs. However, there is limited information on the molecular mechanisms of plant hormones that regulate pod size in peanuts. We identified a mutant with an extremely small pod (*spm*) from Yuanza 9102 (WT) by ^{60}Co γ-radiation mutagenesis. The length and width of the natural mature pod in *spm* were only 71.34% and 73.36% of those in WT, respectively. We performed comparative analyses for morphological characteristics, anatomy, physiology, and global transcriptome between *spm* and WT pods. Samples were collected at 10, 20, and 30 days after peg elongation into the soil, representing stages S1, S2, and S3, respectively. The differences in pod size between WT and *spm* were seen at stage S1 and became even more striking at stages S2 and S3. The cell sizes of the pods were significantly smaller in *spm* than in WT at stages S1, S2, and S3. These results suggested that reduced cell size may be one of the important contributors for the small pod in *spm*. The contents of indole-3-acetic acid (IAA), gibberellin (GA), and brassinosteroid (BR) were also significantly lower in *spm* pods than those in WT pods at all three stages. RNA-Seq analyses showed that 1,373, 8,053, and 3,358 differently expressed genes (DEGs) were identified at stages S1, S2, and S3, respectively. Functional analyses revealed that a set of DEGs was related to plant hormone biosynthesis, plant hormone signal transduction pathway, and cell wall biosynthesis and metabolism. Furthermore, several hub genes associated with plant hormone biosynthesis and signal transduction pathways were identified through weighted gene co-expression network analysis. Our results revealed that IAA, GA, and BR may be important regulators in controlling pod size by regulating cell size in peanuts. This study provides helpful information for the understanding of the complex mechanisms of plant hormones in controlling pod size by regulating the cell size in peanuts and will facilitate the improvement of peanut breeding.

Corresponding authors
Xinyou Zhang, haasxinyou@163.com
Suoyi Han, suoyi_han@126.com

INTRODUCTION

Cultivated peanut (*Arachis hypogaea* L., $2n = 4x = 40$, AABB) is one of the most important oil crops for the human diets worldwide (*Zhuang et al., 2019*). There has been an increasing demand for oil in recent years, highlighting the need for peanut cultivars with high yields (*Wan et al., 2017*). The peanut yield is directly proportional to pod weight, seed weight, and the number of pods per plant (*Gangurde et al., 2020*). Pod size is closely associated with pod weight (*Luo et al., 2018*) and directly affects peanut yield (*Chen et al., 2016*). However, specific peanut pod/seed sizes are preferred by different sectors of industry—bigger is not always acceptable. A comprehensive understanding of the molecular mechanisms governing the pod size and mining the key regulatory factors are crucial for improving pod-related traits in peanuts.

Fruit size is one of prominent agronomical traits for crop domestication and improvement (*Hussain et al., 2020*). Many genes and several pathways/mechanisms involved in fruit size have been identified in several plants, such as *Hyp O-galactosyltransferase* (*HPGT1*) in Arabidopsis (*Ogawa-Ohnishi & Matsubayashi, 2015*), *BnDA1* in rapeseed (*Wang et al., 2017*), *Grain width 2* (*GW2*) in rice (*Yamaguchi et al., 2020*), *Salt and drought-induced RING finger1* (*TaSDIR1-4A*) in wheat (*Wang et al., 2020*), and *KERNEL NUMBER PER ROW 6* (*KNR6*) in maize (*Jia et al., 2020*). Several genes related to plant hormones have been reported to regulate organ size in different plants. *Hussain et al. (2020)* summarized the hormone-related genes involved in regulating fruit size and discussed the pathways/mechanisms. In Arabidopsis, the overexpression of the *AUXIN-REGULATED GENE INVOLVEDIN ORGAN SIZE* (*ARGOS*) gene increased cell size and cell number, resulting in enlarged leaves and siliques (*Wang et al., 2009*). *AUXIN RESPONSE FACTOR 18* (*ARF18*) encodes an auxin-response factor, and disfunction of the *ARF18* gene can induce longer siliques by accelerating cell expansion in the silique wall of *Brassica napus L.* (*Liu et al., 2015*). *GA 20-oxidases* (*GA20ox*) genes, *GA20ox1* and *GA20ox2*, involved in gibberellin (GA) biosynthesis, regulate hypocotyl, internode, and siliques elongation in Arabidopsis (*Rieu et al., 2008*). *TaCYP78A3* encodes a cytochrome P450 CYP78A3, and disfunction of the *TaCYP78A3* can cause a decrease in wheat seed size (*Ma et al., 2015*). The *GRAIN LENGTH2* (*GL2*) is allelic to *GROWTH REGULATION FACTOR4* (*OsGRF4*) and positively regulates brassinosteroid (BR) responses to promote rice grain development (*Che et al., 2015*).

Several major quantitative trait loci (QTLs) related to peanut pod size have been reported in recent years (*Huang et al., 2015*; *Chen et al., 2016*; *Luo et al., 2017*; *Luo et al., 2018*; *Alyr et al., 2020*; *Chu et al., 2020*; *Gangurde et al., 2020*). *Luo et al. (2017)* identified three major QTLs for hundred-pod weight (HPW), pod length and width (PL and PW), which were co-localized in the same region on chromosome A05. Furthermore, *Luo et al. (2018)* co-localized two major QTLs controlling PL and HPW in the same interval on chromosome A05, and three major QTLs for PL, PW, and HPW in the same interval on chromosome A07. *Chu et al. (2020)* identified one major QTL for pod-related traits in a 9 Mbp interval on linkage group A05. *Alyr et al. (2020)* identified one QTL associated with pod and seed size in a 168.37 kb interval on chromosome A07. *Gangurde et al. (2020)*

identified 44 major effect QTLs related to PW and SW in two nested-association mapping populations, and found that most of the QTLs distributed on chromosomes A05, A06, B05, and B06.

Peanut has an unique characteristic of fruit production. It accomplishes flowering and fertilization aerially, but forms the fruits underground (*Smith, 1950*). After fertilization, the peanut gynophore harboring embryo elongates, and forms a special peg-like structure that eventually pushes the embryo into the soil for underground pod development (*Xia et al., 2013*). The pre-embryo develops into a globular embryo after approximately 9 days after peg elongation into the soil (DAP) and the pod becomes enlarged (*Zhang et al., 2016*). Pod development then undergoes rapid growth and expansion during 10–25 DAP. The pod reaches its final size during 25–30 DAP. Previous studies have shown that plant hormones such as auxin (*Moctezuma & Feldman, 1998*; *Moctezuma & Feldman, 1999*; *Moctezuma, 1999*), gibberellin (*Lee, Ketring & Powell, 1972*; *Shushu & Cutter, 1990*), cytokinin (*Shushu & Cutter, 1990*), and ethylene (*Shlamovitz, Ziv & Zamski, 1995*) play important roles in gynophore elongation and pod development in peanut (*Moctezuma, 2003*). There has been increased interest in transcriptome research related to pod development in peanut recently (*Clevenger et al., 2016*; *Li et al., 2017*; *Wan et al., 2017*; *Sinha et al., 2020*; *Yang et al., 2020*). *Clevenger et al. (2016)* constructed a developmental transcriptome map using 22 different tissue types and ontogenies, including a complete reproductive series from flower to fully mature seed, and annotated 21 developmental co-expression networks. *Wan et al. (2017)* conducted transcriptome analyses at three pod developmental stages in peanut and identified two candidate genes related to lignin responsible for pod width. *Sinha et al. (2020)* provided a comprehensive transcriptome map using 20 diverse tissues, and provided insights on gene expression patterns of seed development, photomorphogenesis, allergens, gravitropism, and oil biosynthesis. *Yang et al. (2020)* revealed the molecular mechanism of calcium on peanut pod development by using transcriptome analysis. However, the molecular mechanisms of plant hormones regulation pod size in peanut are still not well understood.

In the present study, we identified a mutant with an extremely small pod (*spm*) from Yuanza 9102 (WT) using ^{60}Co γ-radiation mutagenesis, and performed morphological, anatomical, physiological, and transcriptome analyses for pods in WT and *spm* at three key pod developmental stages. The comparative analyses revealed significant differences in the pod size, cell size, contents of plant hormones, and dynamic gene expression between WT and *spm*. Pairwise comparisons and WGCNA analyses identified several plant hormone-related genes, which were involved in determining peanut pod sizes. Our study contributes to the understanding of the transcriptome dynamics of peanut pod development and are helpful for elucidating the complex regulatory mechanism of pod size in peanuts.

MATERIALS & METHODS

Plant materials and RNA sample collection

The peanut *spm* mutant was selected from an ^{60}Co γ-radiation-induced population originating from Yuanza 9102 (WT). The *spm* mutant was self-pollinated for 10 generations

to ensure a stabilized line for this study. Both WT and *spm* mutant were grown in 2019 in the Yuanyang experiment station of the Henan Academy of Agricultural Sciences. Days to first flower, we marked the flowers and tied the elongating aerial pegs with colored tags (*Yin et al., 2013*). We then artificially covered the tagged pegs with soil to ensure that all pegs elongation into the soil on the same day. Pods were harvested at 10, 20, and 30 days after peg elongation into the soil, which were designated as stages S1, S2, and S3. Three pods from one plant were pooled as one biological replicate, and three different plants represented three biological replicates. All pods were immediately frozen in liquid nitrogen and then stored at −80 °C for RNA isolation.

Trait measurements

The pod and seed traits, including length, width, and weight, were measured as described in *Jiang, Duan & Ren (2006)*. A total of 15 naturally matured dry pods and seeds from five individual plants were harvested. A total of 30 pods were sampled from the tagged pegs of ten individual plants from stages S1, S2, and S3, respectively. These pods were then used to measure pod and seed traits.

Microscopic analyses

Peanut pericarps were collected at stages S1, S2, and S3, and immediately fixed at 4 °C in 2.5% glutaraldehyde in 0.2 M phosphate buffer (pH = 7.3–7.4) for 24 h. Pericarps were dehydrated in an ethanol series (75% for 4 h, 85% for 2 h, 90% for 2 h, 95% for 1 h, and 100% for 1 h). Pericarps were then processed in xylene for 10 min and embedded in paraffin (*Chen et al., 2013*). The pericarps were cut with a rotary microtome (RM2016, Leica) to a 4 µm thickness. The samples were stained with safranin O/fast green and scanned using NIKON ECLIPSE E100 microscope.

Plant hormone quantifications

All the pods of *spm* and WT used for indole-3-acetic acid (IAA), BR, and GA quantification were sampled from the same plants used for RNA-seq at stages S1, S2, and S3. A detailed method for pod collection and store was described in the RNA sample collection. The method for extraction, purification, and quantification of the IAA, BR, and GA by enzyme-linked immunosorbent assay kits was modified following the protocol described in *Wang et al. (2012)*. Differences in plant hormones concentrations between *spm* and WT pods were tested using ANOVA.

RNA-seq and differential genes expression analyses

Total RNA from the marked pod harvested at stages S1, S2, and S3 was extracted using the TRIzol reagent kit (Invitrogen, CA, USA). RNA integrity and quality were tested by using an Agilent 2100 bioanalyzer (Agilent Technologies, CA, USA). Subsequently, a total of 18 libraries were constructed, and the transcriptome sequencing was performed on Illumina HiSeq2500 platform by the Genedenovo Biotechnology Company (Guangzhou, China). The RNA-seq sequencing data in this study have been uploaded to China National Center for Bioinformation under BioProjects, PRJCA006624 (GSA: CRA005103, https://www.cncb.ac.cn/gsa). Low-quality bases and adaptor sequences were eliminated

through fastp (v0.18.0; *Chen et al., 2018*). The remaining sequences were mapped to the ribosome RNA (rRNA) database using Bowtie 2 (v2.2.8; *Langmead & Salzberg, 2012*), and the rRNA mapped sequences were filtered out. The high-quality sequences were aligned to the tetraploid peanut reference genome Tifrunner.gnm1.KYV3 (*Bertioli et al., 2019*; https://peanutbase.org) using HISAT (v2.0.0; *Kim, Langmead & Salzberg, 2015*). Transcripts were assembled and the fragments per kilobase per million reads (FPKM) values were calculated using StringTie (v1.3.1; *Pertea et al., 2015*). Principal component analysis (PCA) was conducted using 'prcomp' utilities in R package. The differential expression between two genotypes at each developmental stage was performed using DESeq2 (*Love, Huber & Anders, 2014*). The differentially expressed genes (DEGs) with the false discovery rate (FDR) < 0.05 and the absolute fold change ($|FC|$) $\geq$ 2 were identified. Gene Ontology (GO), the Kyoto Encyclopedia of Genes and Genomes (KEGG), and MapMan analyses were performed for functional analysis of DEGs as previously described in *Dun et al. (2016)*. The terms/pathways in GO and KEGG analyses with a *q*-value (FDR) < 0.05 were considered to be significantly enriched. The MapMan categories with significance value < 0.05 were used for performing pathway enrichment analysis of DEGs.

Weighted gene co-expression network analysis (WGCNA)

WGCNA was performed for analyzing gene correlation patterns among different samples using the WGCNA software package as described in *Langfelder & Horvath (2008)*. The highly co-expressed gene modules were inferred with a power β of 8, a minimal module size of 50, and a merge-CutHeight of 0.9 after removing the low-quality genes with unstable effects on the results were removed. Association of modules and the particular samples was evaluated using the module eigengene value. The interaction network of genes in modules was visualized using Cytoscape (v3.7.1; *Shannon et al., 2003*).

Quantitative real-time PCR (qRT-PCR)

qRT-PCR analysis was performed using the same pod samples as those used for RNA-seq. The gene-specific primers for qRT-PCR were listed in Table S1. qRT-PCR was conducted using an ABI QS5 (ABI, USA) with SYBR Green detection (TIANGEN, Beijing, China). The actin gene in peanut was used as internal reference for normalizing expression levels of nine genes through the $2^{-\Delta\Delta Ct}$ method (*Livak & Schmittgen, 2001*).

RESULTS

Morphological, anatomical, and physiological analyses on pods at three developmental stages of WT and *spm*

Yuanza 9102 (WT) and its small pod mutant (*spm*), which differ significantly in pod size/weight, were selected to investigate the pod differences (Fig. 1A). The mature dry pod and seed sizes of WT, including length and width, were significantly greater ($P < 0.001$) than those of *spm* (Fig. 1B). The length and width of the pod decreased from 28.12 and 14.60 mm in WT to 20.06 and 10.71 mm in *spm*, respectively. Meanwhile, the length and width of the seed decreased from 14.26 and 10.02 mm in WT to 10.24 and 7.71 mm in *spm*, respectively. The dry weights of the pod, seed, and hull in WT were approximately 3.50-,
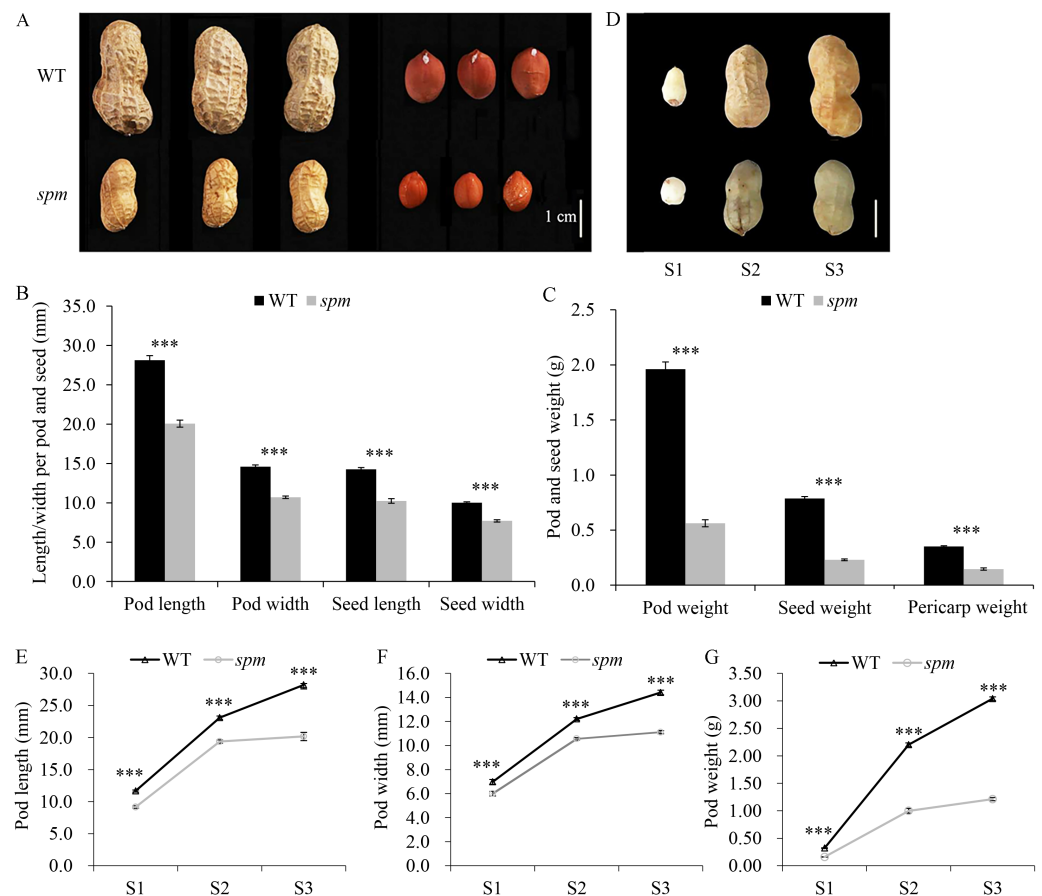
Figure 1 Pod phenotypes at different developmental stages in WT and *spm*. (A) Phenotypes of mature dry peanut pod and seed in WT and *spm*. (B) The mature dry pod and seed length/width in WT and *spm*. (C) The mature dry pod and seed weight in WT and *spm*. (D) Phenotypic characterizations of WT and *spm* pods at three different developmental stages. The samples were collected at 10, 20, and 30 days after peg elongation into the soil (DAP) in WT and *spm*, and the three different developmental stages were designated as stages S1–S3. (E–G) Physical measurements in pod length (E), pod width (F), and pod weight (G) of WT and *spm* at three different developmental stages. The trait values were presented as mean ± SE. The asterisk showed the significant difference between WT and *spm* (t-test; *, $P < 0.05$; **, $P < 0.01$; ***, $P < 0.001$).

3.43-, and 2.50-times as much as those in *spm*, respectively (Fig. 1C). The differences in pod size and weight between WT and *spm* at 10, 20, and 30 DAP were also analyzed. The three stages of pod development were designated as stages S1–S3 (Fig. 1D). Both WT and *spm* pods grew rapidly from stages S1 to S2, but slowly from stages S2 to S3 (Figs. 1E–1G). The rate of increase for pod weight in *spm* was always slower than that in WT from stages S1 to S3 (Fig. 1G). Finally, the pod weight increased 6.56 times in *spm*, but increased 10.69 times in WT from stages S1 to S3. The growth rate for pod size in *spm* was similar to that in WT from stages S1 to S2, but was slower in *spm* than in WT from stages S2 to S3 (Figs. 1E and 1F). The pod size increased 1.20 times and 0.85 times in length and width, respectively, in *spm*, and 1.42 times and 1.06 times in length and width respectively, in WT, from stages

S1 to S3. The differences in pod size and weight between WT and *spm* were seen at stage S1 and were even more pronounced at stages S2 and S3 (Figs. 1E–1G). At stage S1, the pod length, width, and weight of WT were 27.65%, 16.53%, and 62.50% more than those of *spm*, respectively. At stage S2, WT showed 19.26%, 15.63%, and 120% increases in pod length, width, and weight compared with *spm*, respectively. At stage S3, the pod length, width, and weight of WT were 39.93%, 29.70%, and 151.24% more than those of *spm*, respectively.

The anatomical structures of the pod cell, including the exocarp, mesocarp, and endocarp, were analyzed to investigate the cellular differences between WT and *spm*. The results showed that the cell areas increased from stages S1 to S2 in both samples (Figs. 2A–2E). The cell areas were difficult to calculate due to the cell disruption of the mesocarp and endocarp at stage S3. The exocarp cell areas increased approximately 1.50 times in *spm* and WT from stages S1 to S3, the mesocarp cell areas increased approximately 1.00 times in *spm* and WT from stages S1 to S2, and the endocarp cell areas increased approximately 2.28 times and 4.51 times in *spm* and WT from stages S1 to S2, respectively. The exocarp cell areas in *spm* were significantly smaller than those in WT at stages S1 ($P = 0.007$) and S2 ($P = 0.002$). Similarly, the mesocarp cell areas in *spm* were significantly smaller than those in WT at stages S1 ($P < 0.001$) and S2 ($P = 0.002$). The cell areas of *spm* in the endocarp were always significantly smaller ($P < 0.001$) than those of WT from stages S1 to S2 (Fig. 2E). These results suggested that a reduction in cell size may result in decreased pod size in *spm*.

In order to determine the influence of plant hormones on pod size, we measured the contents of several important growth hormones (IAA, GA, and BR) in WT and *spm* pods at three stages. The results showed that the *spm* pods had strikingly lower contents of IAA, GA, and BR than the WT pods at all three stages (Fig. 3), indicating that IAA, GA, and BR may be important for controlling pod size.

RNA-Seq analyses on pods at three developmental stages of WT and *spm*

RNA-Seq analyses were performed at stages S1, S2, and S3 with three independent biological replicates to understand the genetic mechanism of the morphological differences in the pods of WT and *spm*. A total of 18 samples were sequenced, and 35.80–67.65 million high-quality reads were obtained for each sample (Table 1). Approximately 67.83%–97.83% of the high-quality reads were mapped to the peanut tetraploid genome Tifrunner.gnm1.KYV3, and 71,433 genes, including 67,124 known and 4,309 novel genes, were obtained. Genes with FPKM < 0.1 in all samples were removed, and 44,346, 43,737, and 42,146 genes were detected at stages S1, S2, and S3 in WT, respectively. Similarly, 43,606, 41,084, and 41,435 genes were identified at stages S1, S2, and S3 in *spm*, respectively. The number of genes with very high expression levels (FPKM ≥ 50) accounted for approximately 4% in different samples. Approximately 20%, 40%, and 36% of genes with high ($10 \leq$ FPKM < 50), moderate ($2 \leq$ FPKM < 10), and low ($0.1 \leq$ FPKM < 2) expression levels, respectively, were identified in different samples (Fig. 4A).
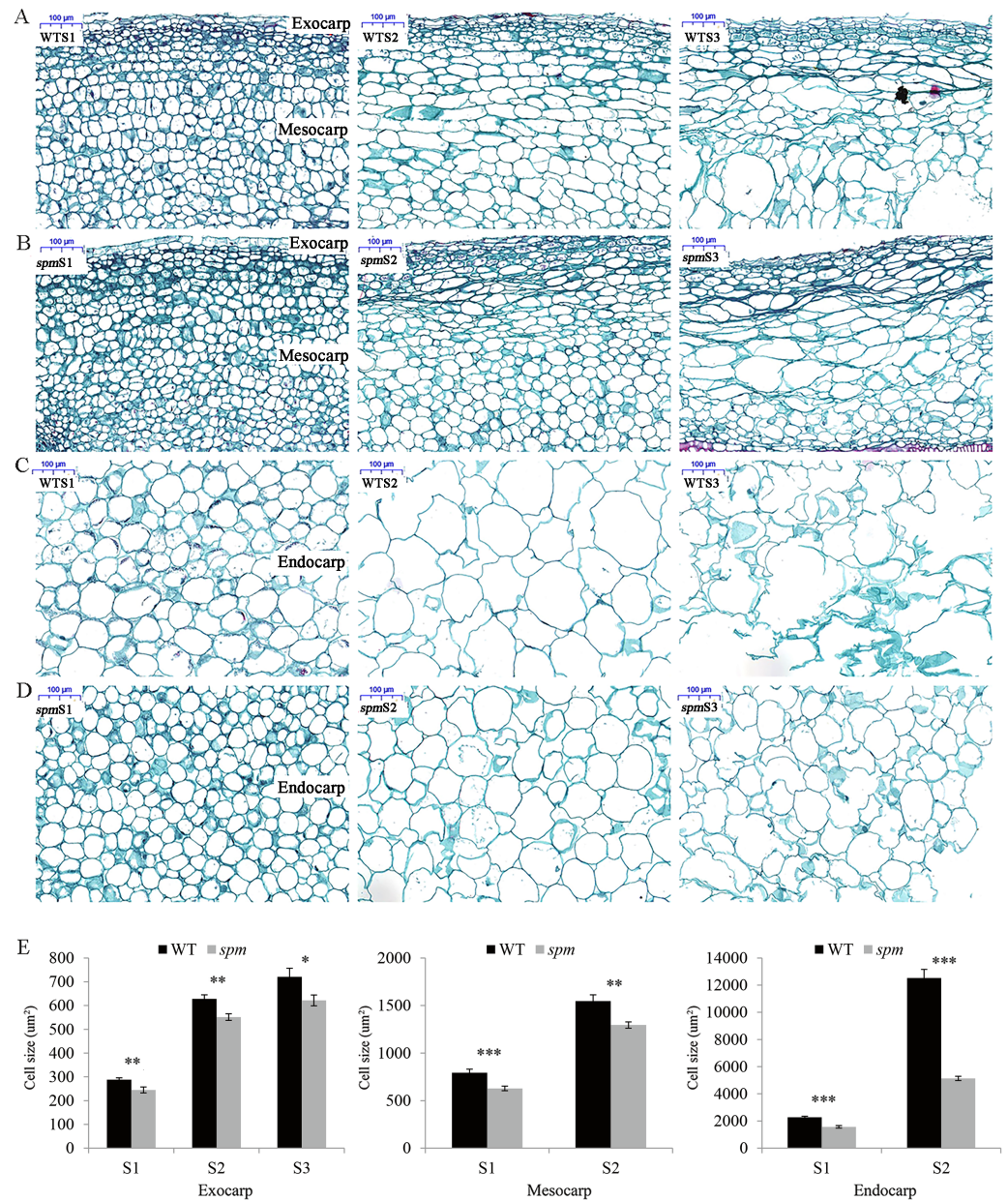
Figure 2 **Transverse sections of pods in WT and *spm*.** (A–D) The transverse sections of the exocarp, mesocarp, and endocarp in WT and *spm* pods from stages S1–S3. WTS1, WTS2, and WTS3 indicated stages S1, S2, and S3 of WT pods, respectively. Similarly, *spm*S1, *spm*S2, and *spm*S3 indicated stages S1, S2, and S3 of *spm* pods, respectively. (E) The average areas of pod cells in unit view. Three unit views were selected to measure cell areas and values were presented as mean ± SE. The asterisk showed a significant difference between WT and *spm* (t-test; *, $P < 0.05$; **, $P < 0.01$; ***, $P < 0.001$).

PCA was performed on 18 samples to better understand the transcriptome dynamics of pod development in WT and *spm* (Fig. 4B). The samples from two genotypes at stage S1 were closely grouped but showed somewhat distinct transcriptional activity. Striking differences were observed in WT and *spm* at stage S2. The WT pod transcriptome at
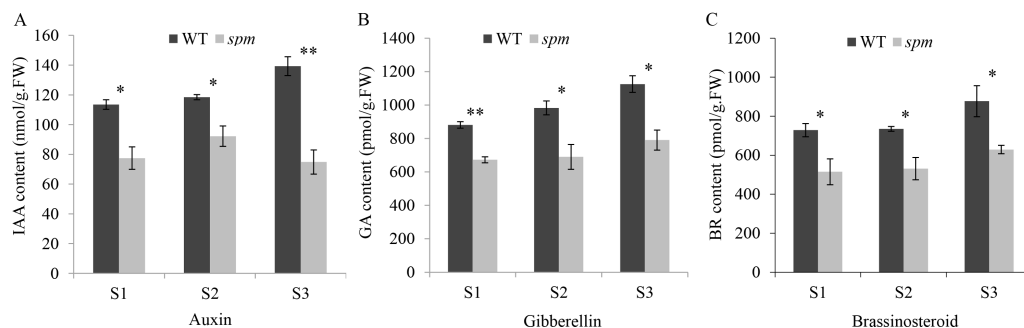
Figure 3 **The contents of plant hormones in the *spm* and WT pods from stages S1–S3.** (A) The IAA contents in the *spm* pods were significantly lower than in WT pods from stages S1–S3 (S1: $P = 0.012$, S2: $P = 0.021$, S3: $P = 0.003$). (B) The GA contents were significantly lower in the *spm* pods than in WT pods from stages S1–S3 (S1: $P = 0.001$, S2: $P = 0.026$, S3: $P = 0.013$). (C) The BR contents were significantly lower in the *spm* pods than in WT pods from stages S1–S3 (S1: $P = 0.045$, S2: $P = 0.025$, S3: $P = 0.040$). Statistically significant differences were analyzed according to three biological replicates (t-test; *$P < 0.05$; **$P < 0.01$; ***$P < 0.001$).

Table 1 **Summary of RNA-seq reads for WT and *spm*.**

Sample	Stage	Raw data	High-quality reads	Uniquely mapped reads	Total mapped reads
WT-1	S1	50093412	48918128	40473799	47855226
WT-2	S1	69607752	67654356	55076743	65389434
WT-3	S1	44199200	43364394	35244184	41419026
WT-1	S2	42237044	41326932	33873522	39953048
WT-2	S2	47354224	46117086	37815080	44967835
WT-3	S2	44691048	43672758	35843063	42344975
WT-1	S3	43019374	42141746	28862870	34269296
WT-2	S3	41185472	39844756	29440277	35222963
WT-3	S3	45976150	44514214	35417643	42529572
spm-1	S1	39160378	37980574	30608769	36814261
spm-2	S1	40327090	38061154	30448990	37151385
spm-3	S1	42090034	41132622	33867279	40049165
spm-1	S2	38999180	37628332	30678611	36728419
spm-2	S2	44578766	43264764	29754842	35576995
spm-3	S2	45530262	44221988	30884178	36892623
spm-1	S3	44145446	43302766	24637836	29372461
spm-2	S3	37115942	35796026	28857209	34561356
spm-3	S3	43005748	41511116	31935728	38276792

stage S2 was closely clustered to the *spm* pod transcriptome at stage S1, whereas stage S2 of the *spm* pod transcriptome tended toward stage S3 of the *spm* pod transcriptome. This indicated that the temporal development progressed faster in *spm* pods than in WT pods. The pods of both genotypes at stage S3 showed striking differences, indicating that substantial differences still existed in their transcriptional programs.
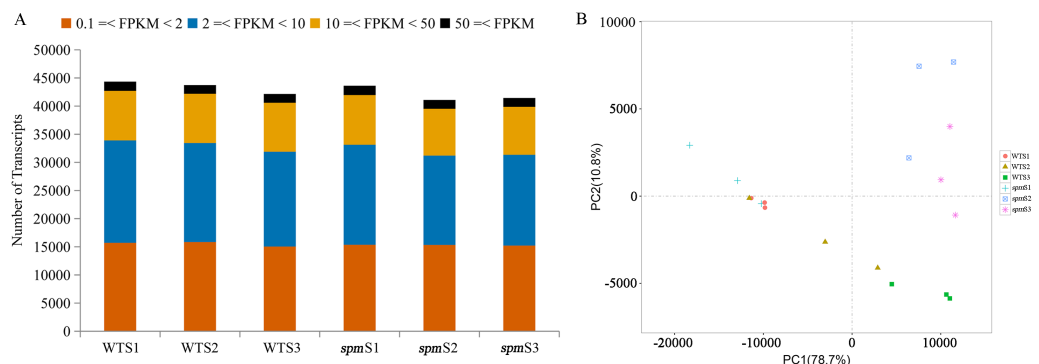
Figure 4 **Gene expression profilings of WT and *spm* pods at three developmental stages.** (A) Numbers of detected transcripts in each pod sample at different developmental stages in WT and *spm*. (B) Principal component analysis (PCA) plots for pod development at different stages in WT and *spm*.

Pairwise comparison at each developmental stage was performed to investigate the transcriptional differences that characterize different pod size in WT and *spm*. A total of 10,396 DEGs ($|FC| \geq 2$ and FDR < 0.05) were detected in *spm* pods compared with WT pods (Fig. 5A). Among these DEGs, 3,734 genes were more highly expressed, and 6,662 genes had lower expression levels in *spm* than in WT. At stage S1, 554 genes were up-regulated and 819 genes were down-regulated in *spm* relative to WT. At stage S2, the number of DEGs peaked, and 8,053 DEGs were detected between *spm* and WT, with 2,664 genes up- and 5,389 genes down-regulated in *spm* relative to WT. At S3 stage, 1,327 genes were up-regulated and 2,031 genes were down-regulated in *spm* compared with WT. Only 62 up-regulated genes overlapped among all three developmental stages in *spm* compared with WT; Stage S1 shared 125 and 111 up-regulated genes with stages S2 and S3, respectively; 637 up-regulated genes overlapped between stages S2 and S3 (Fig. 5B). However, 332 down-regulated genes overlapped at all developmental stages in *spm* compared with WT; 519 down-regulated genes were found between stage S1 and S2, and 353 down-regulated genes were identified between stage S1 and S3; 1,037 down-regulated genes overlapped between stages S2 and S3 (Fig. 5B).

GO enrichment analysis revealed that 80 terms were significantly enriched in biological processes. The term 'carbohydrate metabolic process' was the most enriched, followed by 'small molecule metabolic process', 'organic acid biosynthetic process', 'plant-type cell wall organization', and 'single-organism biosynthetic process' (Fig. 6A, Table S2). Several other biological processes involved in cell wall metabolism were significantly enriched, including, 'DNA-dependent DNA replication', 'microtubule-based process', 'cellular glucan metabolic process', and 'response to biotic stimulus' were also significantly enriched (Table S2). KEGG enrichment analysis was performed, and a total of 103, 131, and 124 pathways were enriched at stages S1, S2, and S3, respectively. Many DEGs at stages S2 and S3 were enriched in 'metabolic pathways', 'plant hormone signal transduction' and 'starch and sucrose metabolism'; however, the numbers of DEGs in these three pathways were remarkably reduced at stage S1 (Fig. 6B). In the 'plant hormone signal transduction'
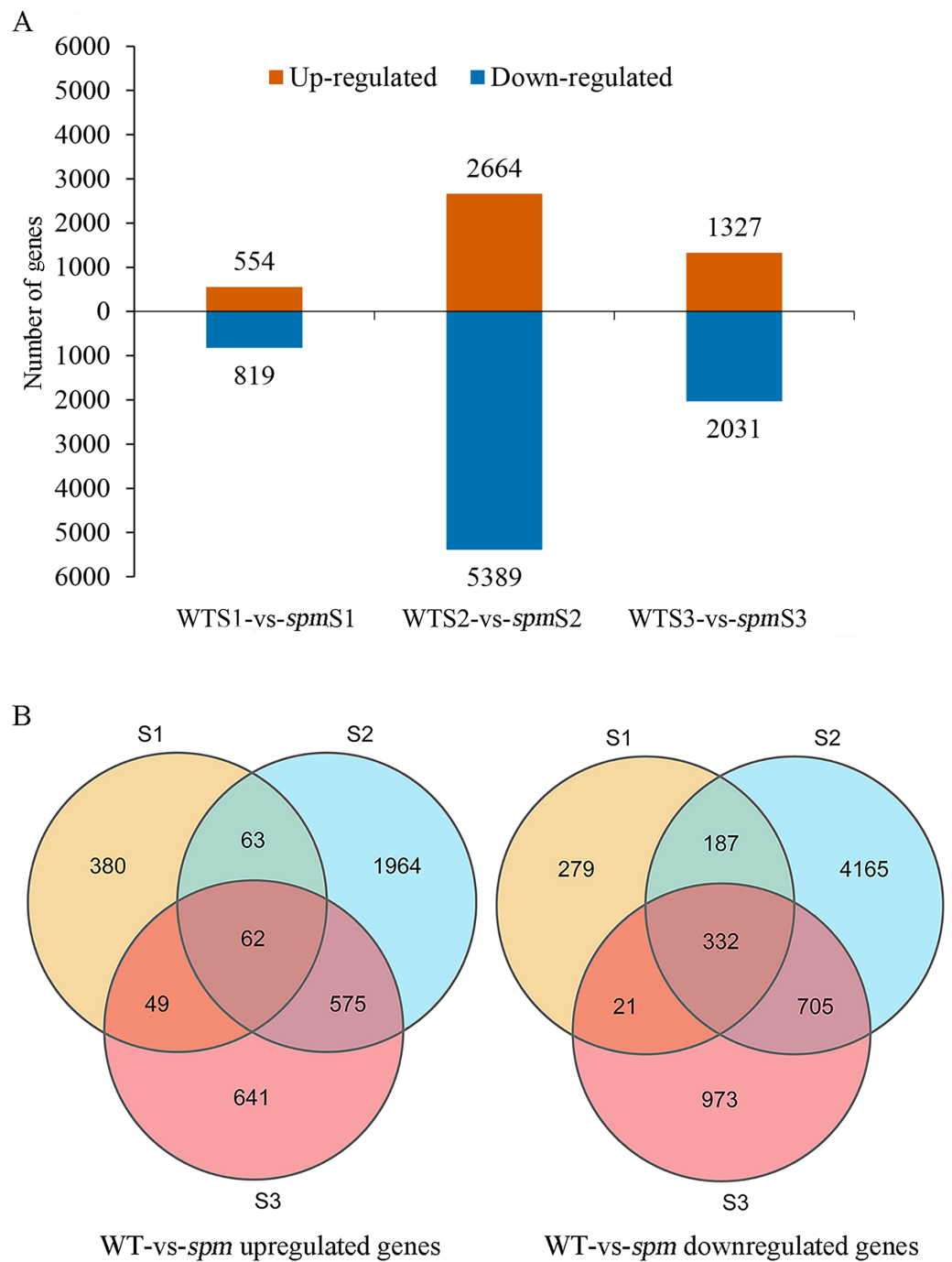
Figure 5 The number of up-regulated and down-regulated genes at each stage of pod development in *spm* as compared with WT. (A) The number of differentially expressed genes from three different stages in WT and *spm*. (B) The overlapping differentially expressed genes between WT and *spm* at three stages.
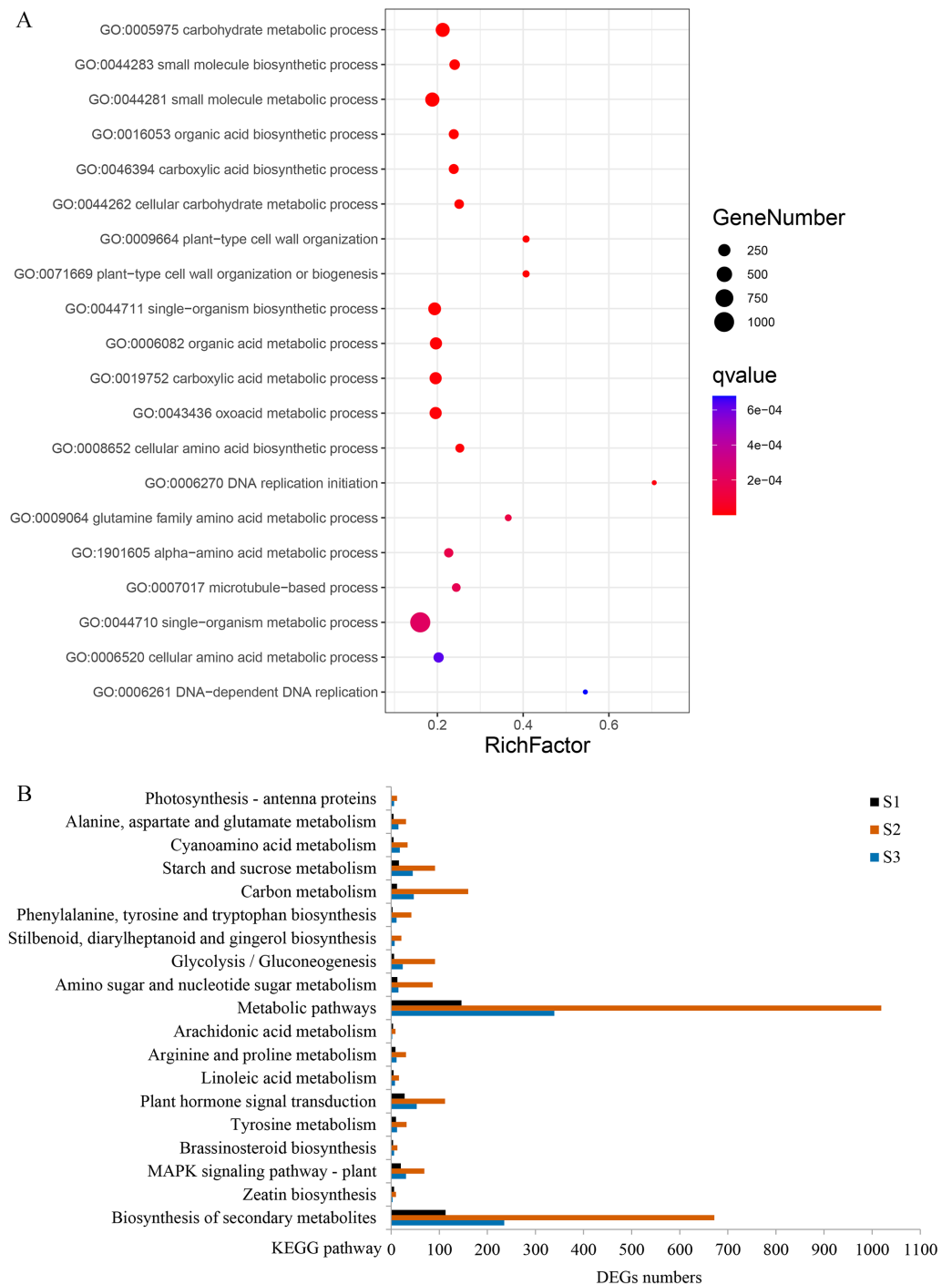
Figure 6 Gene ontology (GO) and Kyoto Encyclopedia of Genes and Genomes (KEGG) enrichment analyses of DEGs between WT and *spm*. (A) The top 20 enriched biological processes for DEGs in the GO enrichment analysis. (B) KEGG pathway enrichment analysis for DEGs at three stages.

pathway, 112 DEGs were enriched, and most of them were up-regulated in WT compared with *spm* at stage S2. These results indicated that genes involved in 'plant hormone signal transduction' have striking differences between WT and *spm* pods at stage S2.

It is noteworthy that a majority of DEGs were identified at stage S2 between WT and *spm*. Furthermore, the numbers of DEGs in the KEGG pathways associated with C and N metabolism peaked at stages S2, indicating that stage S2 may be an important period in pod development. To investigate the metabolic pathways affecting the differences of pod size between WT and *spm* at stage S2, we overlaid the DEGs onto the metabolic pathways using the MapMan. The results showed that the genes in certain metabolic pathways exhibited striking differential expression levels between two genotypes at stage S2 (Fig. 7). For example, the genes involved in starch and sucrose metabolism, cellulose synthesis, cell wall modification, cell division and cell cycle showed higher expression levels in WT (Figs. 7A and 7B), indicating that actively cell expansion and division require higher energy metabolism in WT than in *spm*. In addition, the genes involved in hormone signalling transduction pathway exhibited higher transcriptional activity in WT than in *spm* (Fig. 7B), indicating that plant hormones may be involved in regulating peanut pod size by influencing cell expansion and division.

The expression pattern of cell expansion related genes at stage S2

According to the results of GO analysis, cell expansion-related terms, including 'cell wall organization or biogenesis', 'developmental cell growth', and 'cellulose metabolism process' were significantly enriched at stage S2. In these terms, a total of 48 DEGs encoding xyloglucan endotransglucosylase/hydrolase (XTH), xyloglucan glycosyltransferase (GSLA, GSLC), xyloglucan xylosyltransferase (XXT), cellulose synthase (GESA, GSLD, GSLE, GSLG, and GSLH), and plant invertase/pectin methylesterase inhibitor (PMEI) had significantly lower expression levels in *spm* than in WT at stage S2 (Table S3). These genes are involved in cell wall metabolism, which is crucial for plant cell growth and expansion (*Cosgrove, 2005*; *Liu et al., 2020*). In addition, the genes encoding beta-galactosidase 10 (BGAL10), CLIP-associated protein (CLASP), and LONGIFOLIA 2-like protein (LNG2) showed lower expression levels in *spm* than in WT pods. The *BGAL10* gene is responsible for the majority of b-galactosidase activity against xyloglucan, and disruptions of the *BGAL10* cause growth defects and short silique length (*Sampedro et al., 2012*). The *CLASP* gene encoding a microtubule-associated protein is involved in cell division and expansion (*Ambrose et al., 2007*). The *LNG2* gene positively regulates longitudinal polar cell elongation in Arabidopsis (*Lee et al., 2006*).

The expression pattern of hormones related genes at stage S2

The expression of DEGs related to IAA, GA, and BR showed striking differences at stages S1–S3, especially at stage S2 (Fig. 8). A total of 50 genes exhibited significantly different expression levels in WT and *spm* pods at stage S2 for IAA (Fig. 8A, Table S4). The genes encoding dormancy/auxin-associated family proteins (DRM1), showed significantly higher expression levels in *spm* than in WT at stages S1–S3. The genes encoding protein PIN-LIKES 2 (PILS2) displayed significantly higher expression levels in *spm* than in WT at stages S1 and
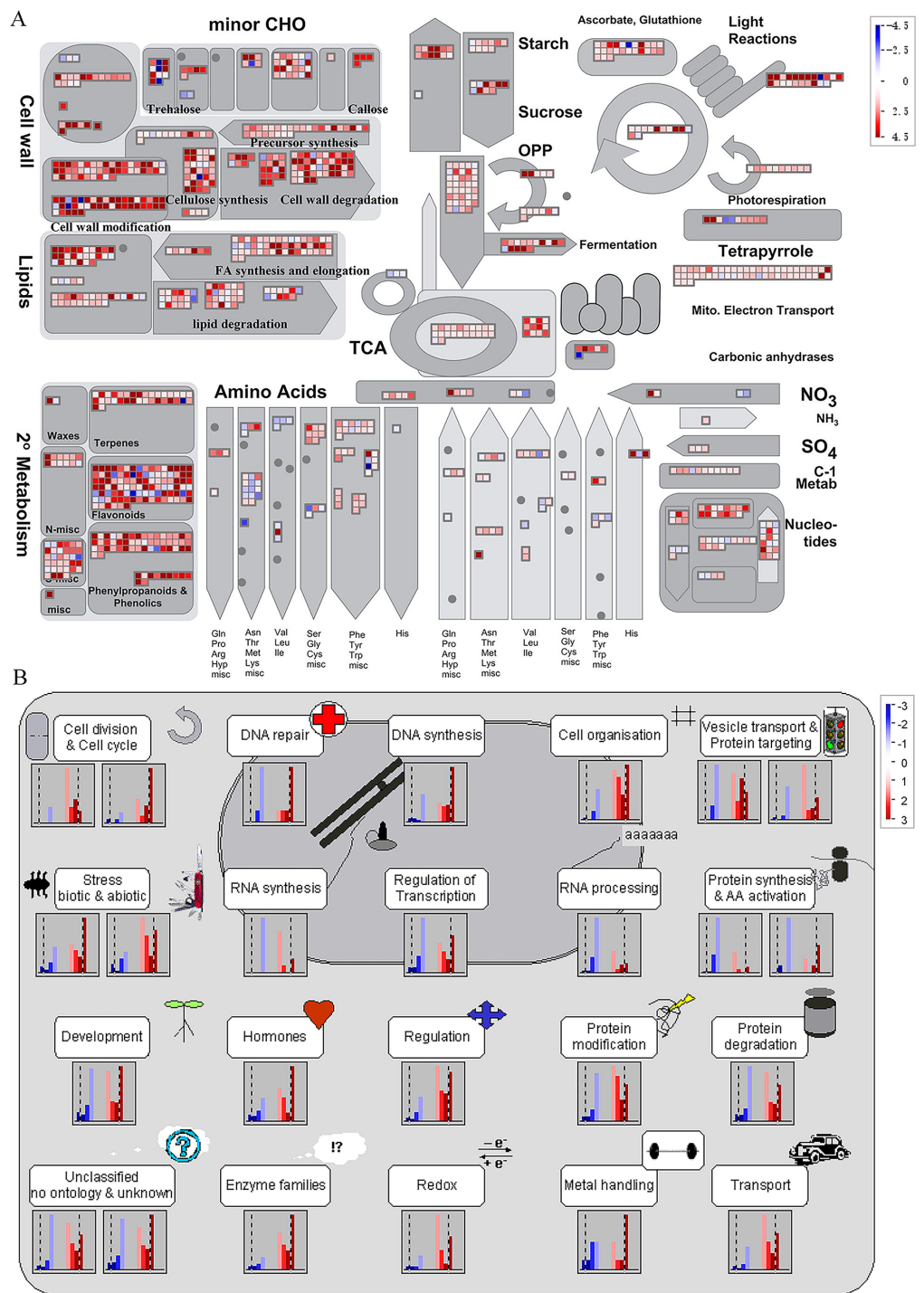
Figure 7 Differential genes expression in *spm* pod as compared with WT pod at stage S2. (A) Metabolic pathways with differential expression profile in *spm* pod as compared with WT pod at S2 stage. (B) Cellular response pathways showing differential expression between *spm* pod and WT pod at stages S2. Differentially expressed genes between *spm* and WT at stage S2 were loaded into MapMan to generate the overview. On the $\log_2$ scale, dark blue and dark red colors represent higher and lower expression, respectively, in *spm* as compared with WT.

Full-size DOI: 10.7717/peerj.12965/fig-7
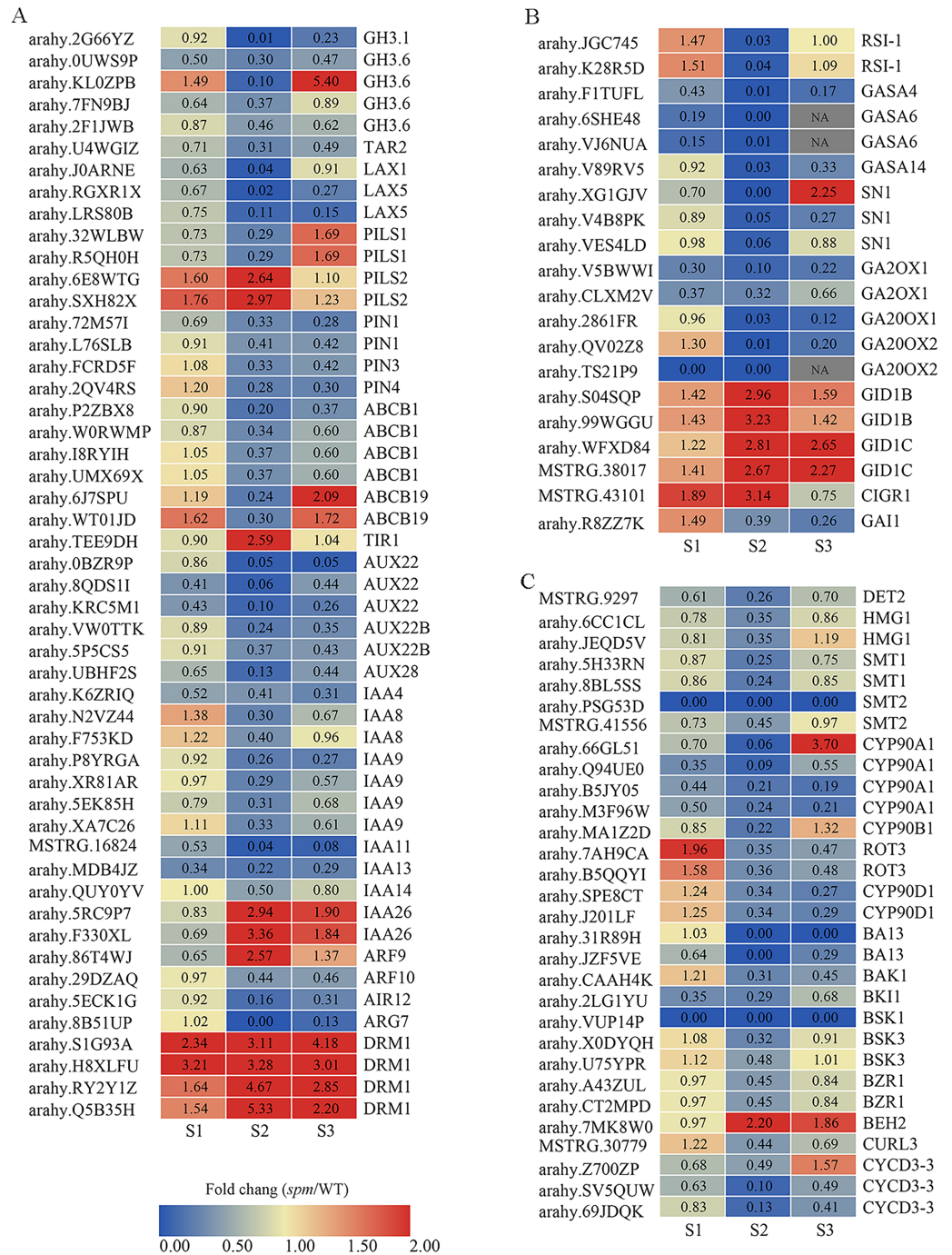
Figure 8 The expression profiles of plant hormones-related genes in *spm* as compared with WT at stages S1–S3. (A) The fold changes (FC) of the auxin-related genes based on the FPKM values in WT and *spm* pods at three developmental stages. (B) The FC of the GA-related DEGs, based on the FPKM in WT and *spm* pods at three developmental stages. (C) The FC of the BR-related DEGs, based on the FPKM in WT and *spm* pods at three developmental stages.

S2, however, *PILS1* genes exhibited significantly lower transcriptional activity in *spm* than in WT at stages S1 and S2. The expression level of gene encoding protein TRANSPORT INHIBITOR RESPONSE 1 (TIR) was significantly higher in *spm* at stages S2. The genes encoding ARF9 and auxin-responsive proteins (IAA26) exhibited significantly higher transcriptional activity in *spm* at stages S2 and S3, whereas other genes encoding ARF10 and Aux/IAA family members (AUX22, AUX22B, AUX28, IAA4, IAA8, IAA9, IAA11, IAA13, IAA14) showed significantly lower expression levels in *spm* at stages S2 and S3. The expression levels of genes encoding tryptophan aminotransferase-related protein 2 (TAR2), ATP-binding cassette subfamily proteins (ABCB1 and ABCB19), auxin-induced in root cultures protein 12 (AIR12), IAA-amido conjugating enzyme family members (GH3.1 and GH3.6), auxin efflux carrier family proteins (PIN1, PIN3 and PIN4), and auxin transporter-like proteins (LAX1 and LAX5) were significantly higher in WT than in *spm* at stage S2.

A total of 20 genes showed strikingly different expression levels between WT and *spm* pods at stage S2 for GA (Fig. 8B, Table S4). The genes encoding gibberellin 2-oxidase 1 proteins (GA2OX1), GA20OX1 and GA20OX2, and DELLA protein GAI1 (GAI1) showed significantly lower transcriptional activity in *spm* compared with WT at stages S2 and S3. The genes encoding GIBBERELLIN INSENSITIVE DWARF1 (GID1B and GID1C) had higher expression levels in *spm* than in WT at three stages. The genes encoding gibberellin-regulated proteins (GASA4, GASA6, GASA14, and SN1) showed significantly lower expression levels in *spm* than in WT at stage S2.

A total of 30 genes exhibited significantly different expression levels between WT and *spm* pod at stage S2 in BR (Fig. 8C, Table S4). Eleven genes encode cytochrome P450 family proteins (CYP90A1, CYP90B1, ROT3, CYP90D1, BA13). Among them, the genes encoding CYP90A1 and CYP90B1 exhibited lower expression levels in *spm* than in WT at stages S1 and S2. Likewise, the transcriptional activity of genes encoding ROT3, CYP90D1, and BA13 was significantly lower in *spm* at stages S2 and S3. The genes encoding BRASSINAZOLE-RESISTANT 1 proteins (BZR1) showed significantly lower expression levels in *spm* than in WT at three stages, whereas, BES1/BZR1 homolog protein 2 (BEH2) showed significantly higher expression levels in *spm* than in WT at stages S2 and S3. The transcriptional activity of genes encoding BRASSINOSTEROID INSENSITIVE 1-associated receptor kinase 1 (BAK1), BRI1 kinase inhibitor 1 (BKI1), Serine/threonine-protein kinase BSK1 (BSK1), and Brassinosteroid LRR receptor kinase (CURL3) was significantly lower in *spm* than in WT at stages S2 and S3. The genes encoding steroid 5-alpha-reductase DET2 (DET2), 3-hydroxy-3-methylglutaryl-coenzyme A reductase-like proteins (HMG1), sterol methyltransferases (SMT1 and SMT2), serine/threonine-protein kinase BSK3 (BSK3), and CYCLIN D3 (CYCD3-3) exhibited significantly lower expression levels in *spm* than in WT at stage S2.

Transcription factors (TFs) involved in pod development

We identified a total of 550 TFs (Table S5) at three different developmental stages of peanut pods using the Plant Transcription Factor Database (*Jin et al., 2017*). Among these TFs, 61 of 98 TFs, 206 of 380 TFs, and 136 of 237 TFs were significantly down-regulated in

Table 2 Transcription factors (TFs) identified in *spm* and WT pods.

TF family	Number of genes	TF family	Number of genes
BHLH	77	C3H	6
MYB	38	CPP	6
MYB-related	25	DBB	5
ERF	34	TCP	5
bZIP	32	ZF-HD	5
C2H2	32	NF-YA	5
NAC	31	Nin-like	5
HD-ZIP	24	SBP	5
WRKY	20	ARR-B	4
Dof	17	RAV	4
HSF	16	WOX	4
LBD	15	BES1	3
Trihelix	14	CO-like	3
G2-like	11	NF-YB	3
B3	10	NF-YC	3
GRAS	10	YABBY	3
FAR1	9	BBR-BPC	2
GRF	9	EIL	2
MIKC	9	LSD	2
TALE	9	HRT-like	1
GATA	8	M-type	1
AP2	7	CAMTA	1
ARF	7	E2F/DP	1
SRS	7	Total	550

spm compared with WT at stages S1, S2, and S3, respectively. These TFs were classified into 47 gene families (Table 2). The BHLH family was the largest, including 77 members, followed by MYB (38 MYB members and 25 MYB-related members), ERF (34 members), bZIP (32 members), C2H2 (32 members), NAC (31 members) and other TFs families (281 members).

WGCNA analysis and identification hub genes associated with pod size

WGCNA analysis was performed to explore the gene co-expression regulation network and identify hub genes that were highly associated with peanut pod size. After removing the low expression of genes (FPKM < 0.5), the remaining 30,233 genes were used to perform WGCNA. According to pairwise correlations of gene expression across all samples, a hierarchical clustering tree with 23 co-expression modules was constructed (Fig. 9A). The correlations between modules and different pod developmental stages were investigated. The results showed that the MM.red and MM.brown modules were highly associated with *spm*S2 and *spm*S3, and the MM.tan module was highly associated with all developmental stages of WT pods (Fig. 9B). The expression pattern of the genes in these three modules
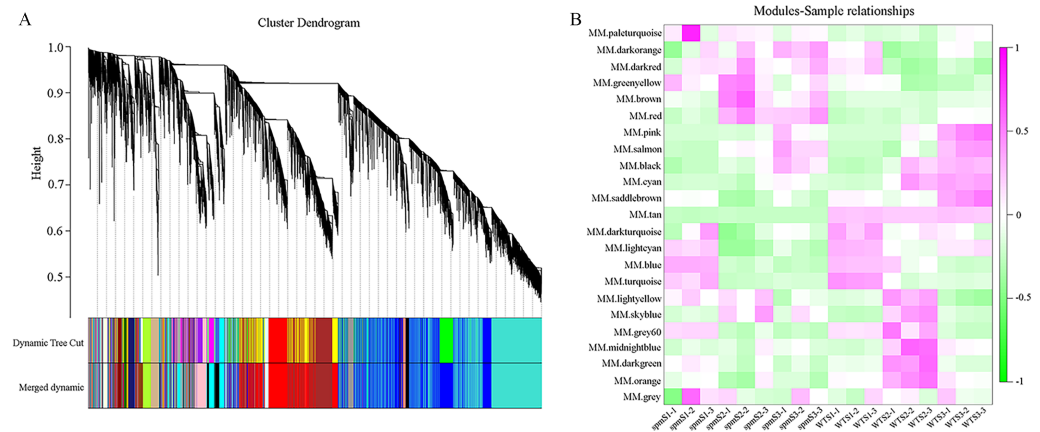
Figure 9 Co-expression network at each pod developmental stage in WT and *spm*. (A) Hierarchical cluster tree of genes based on co-expression network analysis. Each short vertical line in the tree corresponds to one gene. (B) Relationships between co-expressed modules and pod developmental stages in WT and *spm*.

indicated that some genes may play crucial roles in the regulation of peanut pod size (Figs. 10A, 10C and 10E, Table S6). Therefore, the MM.red, MM.brown and MM.tan modules were selected for gene co-expression network analysis to reveal hub genes related to pod size. Hub genes are those that show the most connections in the network (*Du et al., 2017*). Forteen genes from these three modules were identified as hub genes when combined with the results of transcriptome analysis (Figs. 10B, 10D and 10F). Among these genes, *DRM1*, *AIR12*, *AUX22B*, *PILS2*, and *ABCB1* are related to auxin transportation or signal transduction pathways; *GIDIB*, *GIDIC*, and *GA2OX1* are associated with GA biosynthesis or signal transduction pathways; *SMT2*, *BEH2*, *BSK3*, *BSK1*, and *BZR1* are associated with BR biosynthesis or signal transduction pathways. These genes showed differentially expressed levels in *spm* and WT pods at different developmental stages (Fig. 8). These results showed that auxin, GA, and BR biosynthesis and signal transduction pathways may be involved in controlling peanut pod size.

qRT-PCR

Nine hub genes were selected to validate the accuracy of RNA-seq results. These included four genes related to auxin signal transduction pathways, two genes related to GA biosynthesis or signal transduction pathways, and three genes related to BR biosynthesis or signal transduction pathway. The results revealed that the overall expression trend of these nine genes, as quantified by the qRT-PCR, were consistent with those obtained from RNA-seq analysis (Fig. S1), thus demonstrating the reliability of RNA-seq analyses.

DISCUSSION

Fruit size is an important agronomic trait in crop domestication and improvement (*Hussain et al., 2020*). Numerous studies in model plants have shown that plant hormones are crucial for determining fruit size by regulating cell expansion and proliferation
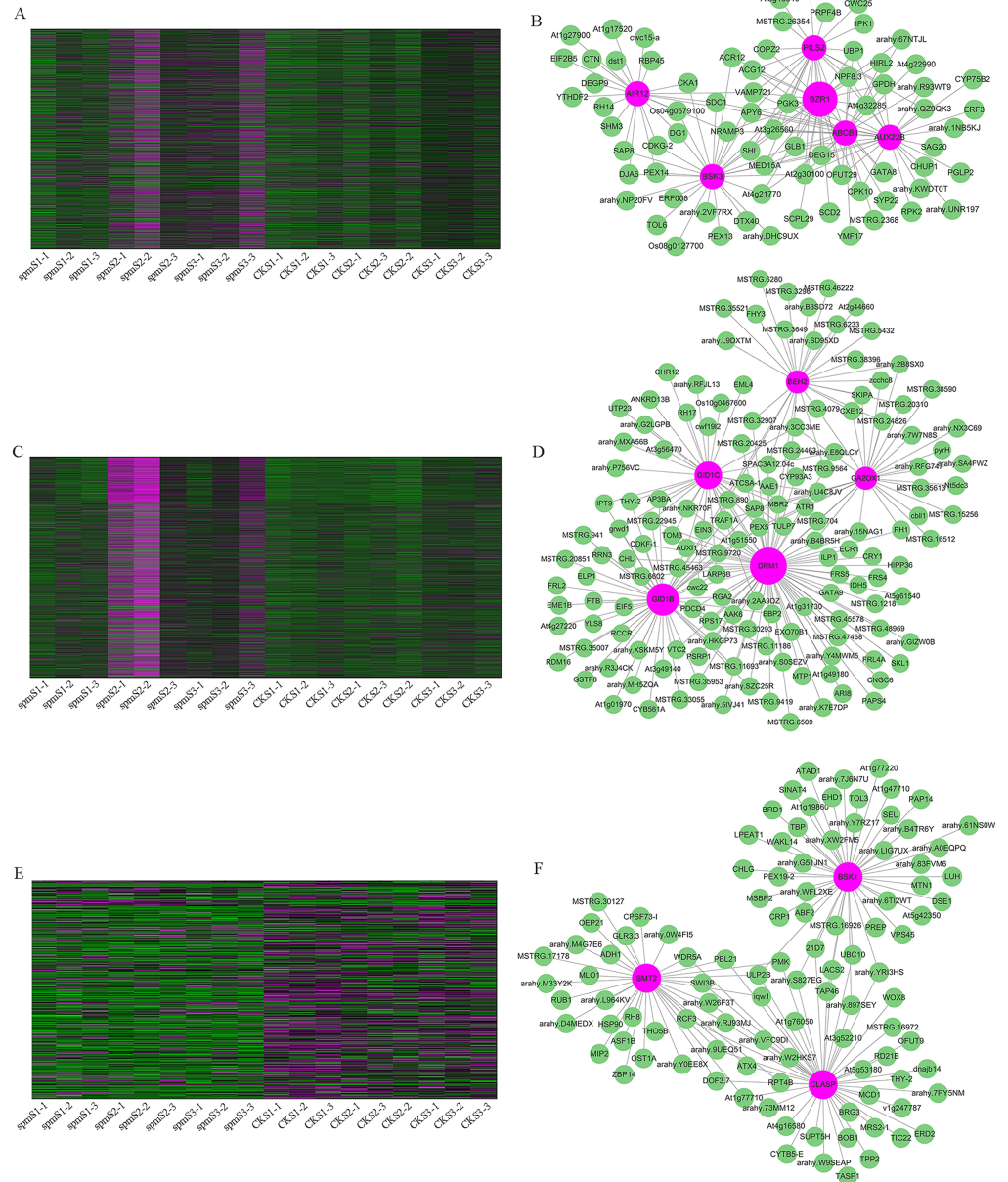
Figure 10 **Co-expression network analysis for three modules.** (A, C, E) Heatmaps of gene expression patterns for MM.red, MM.brown and MM.tan modules. (B, D, F) The correlation networks for MM.red, MM.brown, and MM.tan modules. Candidate hub genes are shown as red nodes.

(*Hussain et al., 2020*; *Fenn & Giovannoni, 2021*). However, the mechanism of plant hormones regulating pod size has been not well understood in peanut. In the present study, we performed phenotype analyses for Yuanza 9102 (WT) and its small pod mutant (*spm*) at three stages. The differences in pod size appeared at stage S1, expanded rapidly at stage S2, and peaked at stage S3 (Figs. 1E–1G). As a result, the mature dry pod size in

spm was strikingly smaller ($P < 0.001$) than in WT (Figs. 1A–1D). Anatomical structure analysis showed that the pod cell sizes were enlarged in both genotypes from stages S1 to S3. However, the cell sizes in *spm* were always smaller than those in WT at three stages, especially at stages S2 and S3 (Figs. 2A–2E). Consistent with the above results, the DEGs related to cell expansion were significantly enriched at stage S2 (Table S3), and most of genes were down-regulated in *spm* compared with WT. Cell size was associated with fruit size (*Cheniclet et al., 2005*; *Liu et al., 2016*), therefore, reduced cell size may be one of important factors for small pods in *spm*. Furthermore, the contents of IAA, GA, and BR in *spm* pods were strikingly lower than those in WT at three stages (Figs. 3A–3C). These hormones are essential to regulate growth, specifically cell elongation (*Depuydt & Hardtke, 2011*). Auxin influences cell division and expansion in developing maize kernels, and auxin deficiency has been shown to result in reduced cell size in the endosperm and a small-seed phenotype (*Bernardi et al., 2012*; *Bernardi et al., 2019*). GA reportedly participated in a wide range of physiological processes, including elongation or expansion of numerous tissues of Arabidopsis (*Rieu et al., 2008*). BR has been shown to be important for cell elongation and division (*Planas-Riverola et al., 2019*). These results indicated that pod size in peanut may be regulated by auxin, GA, and BR, mainly *via* affecting cell expansion. To our knowledge, ours is the first study to report how plant hormones regulate cell expansion to affect pod size in peanut, which may provide a reference for studying the molecular mechanism of peanut pod size.

Though several major QTLs associated with peanut pod size have been identified, the molecular mechanisms of plant hormones regulation pod size are not well understood. We performed comparative analyses for global transcriptome between *spm* and WT pods at stages S1, S2, and S3. KEGG enrichment analyses revealed that a lot of DEGs from three stages were enriched in plant hormone biosynthesis or signal transduction pathways (Fig. 6C). Pairwise comparisons analysis showed that most of DEGs associated with the plant hormone biosynthesis or signal transduction pathways had significantly lower expression levels in *spm* pods than in WT pods (Fig. 8). Furthermore, the results of WGCNA revealed that several hub genes, including *DRM1*, *AIR12*, *AUX22B*, *PILS2*, *ABCB1*, *GIDIB*, *GIDIC*, *GA2OX1*, *SMT2*, *BEH2*, *BSK3*, *BSK1*, and *BZR1*, were involved in auxin, GA, and BR biosynthesis or signal transduction pathways (Fig. 10). These results showed that the plant hormone biosynthesis and signal transduction pathways may play important roles in regulating pod size in peanut.

Several genes related to auxin biosynthesis or signalling pathways have been reported to affect organ growth and development in model plants (*Hussain et al., 2020*). *TAR2*, encoding tryptophan aminotransferase-related protein 2, is involved in the auxin biosynthesis pathway (*Stepanova et al., 2008*). Arabidopsis *TAA1* and *TAR2* double mutation led to multiple organ development deficiencies including dwarfism, reduced vasculature, sterile flowers, and bushy plants with agravitropic roots (*Stepanova et al., 2008*). *Shao et al. (2017)* reported that the overexpression of *TaTAR2.1-3A* in wheat increased plant height, spike number, lateral root branching, and grain yield. A loss-of-function mutation in *TAR2*, *tar2-1*, dramatically reduced the content of IAA and seed size in pea (*McAdam et al., 2017*). Auxin is perceived by a co-receptor complex consisting of

TIR1/AFB and Aux/IAA proteins (*Hayashi et al., 2008*; *Prigge et al., 2020*). Overexpression of *TIR1* gene (*CsTIR1*) decreased seed size and seeds per fruit in cucumber (*Xu et al., 2017*). The gene *DRM1*, which belongs to the auxin-repressed superfamily, negatively regulates *Arabidopsis* petioles and siliques size, probably from suppression of either cell expansion or cell elongation (*Lee, Han & Hur, 2013*). We found that one *TAR2* gene had a significantly lower expression level in *spm* than in WT at stage S2, whereas, the genes *TIR1* and *DRM1*, were significantly up-regulated in *spm* compared with WT at stage S2 (Fig. 8A). These results indicated that *TAR2*, *TIR1*, and *DRM1* may be important regulators for pod size.

Gibberellin is an essential hormone that regulates plant growth and development (*Livne & Weiss, 2014*). The activity of the *GA20ox* is important for GA production and GA-dependent development. *Rieu et al. (2008)* reported that *AtGA20ox1* and *AtGA20ox2* promote hypocotyl, internode, and siliques elongation in Arabidopsis, and *ga20ox2* and *ga20ox1 ga20ox2* mutant siliques were significantly shorter than wild type siliques. In this study, the *GA20ox* genes were significantly down-regulated in *spm* compared with WT at stage S2 (Fig. 8B), indicating that *GA20ox* may positively regulate pod size in peanut by mediating GA biosynthesis. BRs, which are steroidal hormones, play important roles in regulating the cell elongation, cell division, and differentiation of various cell types in plant (*Li et al., 2018*; *Planas-Riverola et al., 2019*). Campesterol is a biosynthetic precursor of BR (*Ohnishi et al., 2006*), and loss the function of sterol-related genes results in dysfunctional BR biosynthesis, resulting in dwarfism in Arabidopsis (*Schrick et al., 2000*; *Schaller, 2004*). The genes *HMG1* encoding 3-hydroxy-3-methylglutaryl-coenzyme A reductase 1 and *SMT2* encoding 24-methylenesterol C-methyltransferase 2 were involved in sterol biosynthesis. The *hmg1* and *smt2* mutants exhibited short siliques in Arabidopsis (*Suzuki et al., 2004*; *Hwang et al., 2007*). In our study, the sterol biosynthesis genes *HMG1*, *SMT1*, and *SMT2* were all down-regulated in *spm* (Fig. 8C). These results suggested that low content of sterol leads to low content of BR, resulting in small pod size in *spm*. As important enzymes in BR biosynthesis, several cytochrome P450 family genes, including *CYP90A1*, *CYP90B1*, *ROT3* and *CYP90D1*, were reported to regulate organ size in Arabidopsis (*Kim, Tsukaya & Uchimiya, 1998*; *Choe et al., 2001*; *Si et al., 2016*). *Choe et al. (2001)* reported that the overexpression of *DWARF4/CYP90B1* resulted in improving BR level and increasing silique length in Arabidopsis. The overexpression of *CYP90A1/CPD* and *DWF4/CYP90B1*, significantly increased silique length and cell size of cortical in Arabidopsis (*Si et al., 2016*). The *ROT3* regulated the polar elongation of cells in leaves of Arabidopsis (*Kim, Tsukaya & Uchimiya, 1998*). *BZR1* is a crucial transcription factor that regulates organ size in the BR signalling pathway in plants (*Zhang et al., 2020*). The overexpression of *ZmBZR1* led to dramatically larger and longer cells in transgenic *ZmBZR1* lines than in WT plants, and the transgenic *ZmBZR1* lines displayed phenotypes of enlarged cotyledons, floral organs, and seed size in Arabidopsis (*Zhang et al., 2020*). Overexpression of the *ZmBES1/BZR1-5* gene resulted in significantly increase of seed size and weight in rice, and smaller kernels produced in maize mutants (*Sun et al., 2021*). In our study, several key BR biosynthetic genes *CYP90A1*, *CYP90B1*, *ROT3* and *CYP90D1* were all down-regulated at stage S2 in *spm*, and *BZR1*, the key transcription factor gene in the BR signalling pathway, was down-regulated in *spm* at all stages (Fig. 8C). Therefore, we speculate that *HMG1*, *SMT2*,

CYP90A1, *CYP90B1*, *ROT3*, *CYP90D1*, and *BZR1* maybe important genes in regulating pod size in peanut.

Plant hormones act synergistically to regulate plant growth and development (*Fenn & Giovannoni, 2021*). Auxin could increase the expression of *CPY90B1* gene resulting in an enhancement in BR biosynthesis (*Chung et al., 2011*). In addition, auxin treatment could increase the expression of BR receptor gene *BRI1* leading to an enhancement in BR perception (*Saini, Sharma & Pati, 2015*). BR also affects polar auxin transport by regulating auxin-responsive genes, such as *PIN2*, and *PIN4* (*Hacham et al., 2012*). The application of 2, 4-D (a synthetic auxin mimic) could induce *GA20ox* and *GA3ox* expression, and promote cell division and expansion (*Cong et al., 2019*). The interplay between BR and GA has also been reported (*Li & He, 2013*; *Vanstraelen & Benková, 2012*). The BZR1 positively regulates expression of *GA20ox* to induce GA biosynthesis and promote cell elongation (*Tong et al., 2014*; *Unterholzner et al., 2015*). These results suggested that significantly down-regulated genes involved in BR/GA biosynthesis and response, and disordered polar auxin transport acted synergistically, leading to small pod size.

CONCLUSIONS

In this study, the pod size and cell size were always smaller in *spm* than in WT at three developmental stages, suggesting that reduced cell size may be one of the important factors for small pod size. A physiological analysis revealed that the contents of IAA, GA, and BR were also lower in *spm* pods than in WT pods at all three stages. We found that many DEGs were associated with cell expansion-related terms and plant hormone signal transduction pathway according to GO and KEGG enrichment analyses. In addition, WGCNA identified several hub genes involved in plant hormone biosynthesis and signal transduction pathways. In summary, the results of our study showed that auxin, GA, and BR may be important regulators in controlling pod size by regulating cell size in peanut. This study promotes our understanding of the complex mechanism of plant hormones in controlling pod size *via* regulating cell size in peanut and may facilitate the improvement of peanut breeding.

Funding
This research was supported by the China Agriculture Research System (CARS-13), the Major Technology Research and Development of Henan Province, China (201300111000), the Henan Provincial Agriculture Research System, China (S2012-5), and the Scientific and Technological Innovation Project of Henan Academy of Agricultural Sciences (2020CX07). The funders had no role in study design, data collection and analysis, decision to publish, or preparation of the manuscript.

Grant Disclosures
The following grant information was disclosed by the authors:

China Agriculture Research System: (CARS-13).
Major Technology Research and Development of Henan Province, China: (201300111000).
Henan Provincial Agriculture Research System, China: (S2012-5).
Scientific and Technological Innovation Project of Henan Academy of Agricultural Sciences: (2020CX07).

Competing Interests

The authors declare there are no competing interests.

Author Contributions

- Yaqi Wang performed the experiments, analyzed the data, prepared figures and/or tables, authored or reviewed drafts of the paper, and approved the final draft.
- Maoning Zhang, Pei Du and Hua Liu performed the experiments, prepared figures and/or tables, and approved the final draft.
- Zhongxin Zhang, Jing Xu and Li Qin performed the experiments, authored or reviewed drafts of the paper, and approved the final draft.
- Bingyan Huang and Xinyou Zhang conceived and designed the experiments, authored or reviewed drafts of the paper, and approved the final draft.
- Zheng Zheng and Wenzhao Dong analyzed the data, authored or reviewed drafts of the paper, and approved the final draft.
- Suoyi Han conceived and designed the experiments, prepared figures and/or tables, authored or reviewed drafts of the paper, and approved the final draft.

Data Availability

The RNA-seq raw data are available in the China National Center for Bioinformation: PRJCA006624, GSA: CRA005103. https://ngdc.cncb.ac.cn/gsa/s/56M3N0K4.

The pod traits and qRT-PCR data and RNA-seq data are also available as Supplemental Files.

Supplemental Information

Supplemental information for this article can be found online at http://dx.doi.org/10.7717/peerj.12965#supplemental-information.

REFERENCES

Alyr MH, Pallu J, Sambou A, Nguepjop JR, Seye M, Tossim HA, Djiboune YR, Sane D, Rami JF, Fonceka D. 2020. Fine-Mapping of a wild genomic region involved in pod and seed size reduction on chromosome A07 in peanut (*Arachis hypogaea* L.). *Genes* **11**(12):1402 DOI 10.3390/genes11121402.

Ambrose JC, Shoji T, Kotzer AM, Pighin JA, Wasteneys GO. 2007. The Arabidopsis *CLASP* gene encodes a microtubule-associated protein involved in cell expansion and division. *Plant Cell* **19**:2763–2775 DOI 10.1105/tpc.107.053777.

Bernardi J, Battaglia R, Bagnaresi P, Lucini L, Marocco A. 2019. Transcriptomic and metabolomic analysis of *ZmYUC1* mutant reveals the role of auxin during early endosperm formation in maize. *Plant Science* **281**:133–145 DOI 10.1016/j.plantsci.2019.01.027.

Bernardi J, Lanubile A, Li QB, Kumar D, Kladnik A, Cook SD, Ross JJ, Marocco A, Chourey PS. 2012. Impaired auxin biosynthesis in the defective endosperm18 mutant is due to mutational loss of expression in the *ZmYuc1* gene encoding endosperm-specific YUCCA1 protein in maize. *Plant Physiology* **160**:1318–1328 DOI 10.1104/pp.112.204743.

Bertioli DJ, Jenkins J, Clevenger J, Dudchenko O, Gao D, Seijo G, Leal-Bertioli SCM, Ren L, Farmer AD, Pandey MK, Samoluk SS, Abernathy B, Agarwal G, Ballén-Taborda C, Cameron C, Campbell J, Chavarro C, Chitikineni A, Chu Y, Dash S, El Baidouri M, Guo B, Huang W, Kim KD, Korani W, Lanciano S, Lui CG, Mirouze M, Moretzsohn MC, Pham M, Shin JH, Shirasawa K, Sinharoy S, Sreedasyam A, Weeks NT, Zhang X, Zheng Z, Sun Z, Froenicke L, Aiden EL, Michelmore R, Varshney RK, Holbrook CC, Cannon EKS, Scheffler BE, Grimwood J, Ozias-Akins P, Cannon SB, Jackson SA, Schmutz J. 2019. The genome sequence of segmental allotetraploid peanut *Arachis hypogaea*. *Nature Genetics* **51**:877–884 DOI 10.1038/s41588-019-0405-z.

Che R, Tong H, Shi B, Liu Y, Fang S, Liu D, Xiao Y, Hu B, Liu L, Wang H, Zhao M, Chu C. 2015. Control of grain size and rice yield by *GL2*-mediated brassinosteroid responses. *Nature Plants* **2**:15195 DOI 10.1038/nplants.2015.195.

Chen WG, Jiao YQ, Cheng LQ, Huang L, Liao BS, Tang M, Ren XP, Zhou XJ, Chen YN, Jiang HF. 2016. Quantitative trait locus analysis for pod- and kernel-related traits in the cultivated peanut (*Arachis hypogaea* L.). *BMC Genetics* **17**:25 DOI 10.1186/s12863-016-0337-x.

Chen S, Zhou Y, Chen Y, Gu J. 2018. fastp: an ultra-fast all-in-one FASTQ preprocessor. *Bioinformatics* **34**:i884–i890 DOI 10.1093/bioinformatics/bty560.

Chen X, Zhu W, Azam S, Li H, Zhu F, Li H, Hong Y, Liu H, Zhang E, Wu H, Yu S, Zhou G, Li S, Zhong N, Wen S, Li X, Knapp SJ, Ozias-Akins P, Varshney RK, Liang X. 2013. Deep sequencing analysis of the transcriptomes of peanut aerial and subterranean young pods identifies candidate genes related to early embryo abortion. *Plant Biotechnology Journal* **11**:115–127 DOI 10.1111/pbi.12018.

Cheniclet C, Rong WY, Causse M, Frangne N, Bolling L, Carde JP, Renaudin JP. 2005. Cell expansion and endoreduplication show a large genetic variability in pericarp and contribute strongly to tomato fruit growth. *Plant Physiology* **139**:1984–1994 DOI 10.1104/pp.105.068767.

Choe S, Fujioka S, Noguchi T, Takatsuto S, Yoshida S, Feldmann KA. 2001. Overexpression of *DWARF4* in the brassinosteroid biosynthetic pathway results in increased vegetative growth and seed yield in Arabidopsis. *Plant Journal* **26**:573–582 DOI 10.1046/j.1365-313x.2001.01055.x.

Chu Y, Chee P, Isleib TG, Holbrook CC, Ozias-Akins P. 2020. Major seed size QTL on chromosome A05 of peanut (*Arachis hypogaea*) is conserved in the US mini core germplasm collection. *Molecular Breeding* **40**:1–16 DOI 10.1007/s11032-019-1082-4.

Chung Y, Maharjan PM, Lee O, Fujioka S, Jang S, Kim B, Takatsuto S, Tsujimoto M, Kim H, Cho S, Park T, Cho H, Hwang I, Choe S. 2011. Auxin stimulates *DWARF4* expression and brassinosteroid biosynthesis in Arabidopsis. *Plant Journal* **66**:564–578 DOI 10.1111/j.1365-313X.2011.04513.x.

Clevenger J, Chu Y, Scheffler B, Ozias-Akins P. 2016. A developmental transcriptome map for allotetraploid *Arachis hypogaea*. *Frontiers in Plant Science* **7**:1446 DOI 10.3389/fpls.2016.01446.

Cong L, Yue R, Wang H, Liu J, Zhai R, Yang J, Wu M, Si M, Zhang H, Yang C, Xu L, Wang Z. 2019. 2, 4-D-induced parthenocarpy in pear is mediated by enhancement of GA4 biosynthesis. *Physiologia Plantarum* **166**:812–820 DOI 10.1111/ppl.12835.

Cosgrove DJ. 2005. Growth of the plant cell wall. *Nature Reviews Molecular Cell Biology* **6**:850–861 DOI 10.1038/nrm1746.

Depuydt S, Hardtke CS. 2011. Hormone signalling crosstalk in plant growth regulation. *Current Biology* **21**:R365–R373 DOI 10.1016/j.cub.2011.03.013.

Du J, Wang S, He C, Zhou B, Ruan YL, Shou H. 2017. Identification of regulatory networks and hub genes controlling soybean seed set and size using RNA sequencing analysis. *Journal of Experimental Botany* **68**:1955–1972 DOI 10.1093/jxb/erw460.

Dun X, Tao Z, Wang J, Wang X, Liu G, Wang H. 2016. Comparative transcriptome analysis of primary roots of *Brassica napus* seedlings with extremely different primary root lengths using RNA sequencing. *Frontiers in Plant Science* **7**:1238 DOI 10.3389/fpls.2016.01238.

Fenn MA, Giovannoni JJ. 2021. Phytohormones in fruit development and maturation. *Plant Journal* **105**:446–458 DOI 10.1111/tpj.15112.

Gangurde SS, Wang H, Yaduru S, Pandey MK, Fountain JC, Chu Y, Isleib T, Holbrook CC, Xavier A, Culbreath AK, Ozias-Akins P, Varshney RK, Guo B. 2020. Nested-association mapping (NAM)-based genetic dissection uncovers candidate genes for seed and pod weights in peanut (*Arachis hypogaea*). *Plant Biotechnology Journal* **18**:1457–1471 DOI 10.1111/pbi.13311.

Hacham Y, Sela A, Friedlander L, Savaldi-Goldstein S. 2012. BRI1 activity in the root meristem involves post-transcriptional regulation of PIN auxin efflux carriers. *Plant Signaling & Behavior* **7**:68–70 DOI 10.4161/psb.7.1.18657.

Hayashi K, Tan X, Zheng N, Hatate T, Kimura Y, Kepinski S, Nozaki H. 2008. Small-molecule agonists and antagonists of F-box protein-substrate interactions in auxin perception and signaling. *Proceedings of the National Academy of Sciences of the United States of America* **105**:5632–5637 DOI 10.1073/pnas.0711146105.

Huang L, He HY, Chen WG, Ren XP, Chen YN, Zhou XJ, Xia YL, Wang XL, Jiang XG, Liao BS, Jiang HF. 2015. Quantitative trait locus analysis of agronomic and quality-related traits in cultivated peanut (*Arachis hypogaea* L.). *Theoretical & Applied Genetics* **128**:1103–1115 DOI 10.1007/s00122-015-2493-1.

Hussain Q, Shi JQ, Scheben A, Zhan JP, Wang XF, Liu GH, Yan GJ, King GJ, Edwards D, Wang HZ. 2020. Genetic and signalling pathways of dry fruit size: targets for genome editing-based crop improvement. *Plant Biotechnology Journal* **18**:1124–1140 DOI 10.1111/pbi.13318.

Hwang I, Paudyal DP, Kim SK, Cheong H. 2007. Influence of the *SMT2* knock-out on hypocotyl elongation in *Arabidopsis thaliana*. *Biotechnology and Bioprocess Engineering* **12**:157–164 DOI 10.1007/BF03028643.

Jia H, Li M, Li W, Liu L, Jian Y, Yang Z, Shen X, Ning Q, Du Y, Zhao R, Jackson D, Yang X, Zhang Z. 2020. A serine/threonine protein kinase encoding gene *KERNEL NUMBER PER ROW6* regulates maize grain yield. *Nature Communications* **11**:988 DOI 10.1038/s41467-020-14746-7.

Jiang H, Duan N, Ren X. 2006. *Descriptors and data standard for peanut (Arachis spp.).* Beijing: China Agriculture Press.

Jin J, Tian F, Yang DC, Meng YQ, Kong L, Luo J, Gao G. 2017. PlantTFDB 4.0: toward a central hub for transcription factors and regulatory interactions in plants. *Nucleic Acids Research* **45**(**D1**):D1040–D1045 DOI 10.1093/nar/gkw982.

Kim D, Langmead B, Salzberg SL. 2015. HISAT: a fast spliced aligner with low memory requirements. *Nature Methods* **12**:357–360 DOI 10.1038/nmeth.3317.

Kim GT, Tsukaya H, Uchimiya H. 1998. The *ROTUNDIFOLIA3* gene of Arabidopsis thaliana encodes a new member of the cytochrome P-450 family that is required for the regulated polar elongation of leaf cells. *Genes & Development* **12**:2381–2391 DOI 10.1101/gad.12.15.2381.

Langfelder P, Horvath S. 2008. WGCNA: an R package for weighted correlation network analysis. *BMC Bioinformatics* **9**:559 DOI 10.1186/1471-2105-9-559.

Langmead B, Salzberg SL. 2012. Fast gapped-read alignment with Bowtie 2. *Nature Methods* **9**:357–359 DOI 10.1038/nmeth.1923.

Lee J, Han CT, Hur Y. 2013. Molecular characterization of the Brassica rapa auxin-repressed, superfamily genes, BrARP1 and *BrDRM1*. *Molecular Biology Reports* **40**:197–209 DOI 10.1007/s11033-012-2050-9.

Lee TA, Ketring DL, Powell RD. 1972. Flowering and growth response of peanut plants (*Arachis hypogaea* L. Var. Starr) at two levels of relative humidity. *Plant Physiology* **49**:190–193 DOI 10.1104/pp.49.2.190.

Lee YK, Kim GT, Kim IJ, Park J, Kwak SS, Choi G, Chung WI. 2006. LONGIFOLIA1 and *LONGIFOLIA2*, two homologous genes, regulate longitudinal cell elongation in Arabidopsis. *Development* **133**:4305–4314 DOI 10.1242/dev.02604.

Li QF, He JX. 2013. Mechanisms of signaling crosstalk between brassinosteroids and gibberellins. *Plant Signaling & Behavior* **8**:e24686 DOI 10.4161/psb.24686.

Li QF, Lu J, Yu JW, Zhang CQ, He JX, Liu QQ. 2018. The brassinosteroid-regulated transcription factors BZR1/BES1 function as a coordinator in multisignal-regulated plant growth. *Biochimca et Biophysica Acta-Gene Regulatory Mechanisms* **1861**:561–571 DOI 10.1016/j.bbagrm.2018.04.003.

Li Y, Meng J, Yang S, Guo F, Zhang J, Geng Y, Cui L, Wan S, Li X. 2017. Transcriptome analysis of calcium- and hormone-related gene expressions during

different stages of peanut pod development. *Frontiers in Plant Science* **8**:1241 DOI 10.3389/fpls.2017.01241.

Liu J, Hua W, Hu Z, Yang H, Zhang L, Li R, Deng L, Sun X, Wang X, Wang H. 2015. Natural variation in *ARF18* gene simultaneously affects seed weight and silique length in polyploid rapeseed. *Proceedings of the National Academy of Sciences of the United States of America* **112**:5123–5132 DOI 10.1073/pnas.1502160112.

Liu JH, Li YC, Zhang J, Gao PZ, Wang AB, Zhang N, Xu BY, Jin ZQ. 2016. Banana *MaEF1A* facilitates plant growth and development. *Biologia Plantarum* **60**:435–442 DOI 10.1007/s10535-016-0613-7.

Liu J, Shi M, Wang J, Zhang B, Li Y, Wang J, El-Sappah AH, Liang Y. 2020. Comparative transcriptomic analysis of the development of sepal morphology in tomato (*Solanum Lycopersicum* L.). *International Journal of Molecular Sciences* **21**:5914 DOI 10.3390/ijms21165914.

Livak KJ, Schmittgen TD. 2001. Analysis of relative gene expression data using real-time quantitative PCR and the 2(−Delta Delta C(T)) Method. *Methods* **25(4)**:402–408 DOI 10.1006/meth.2001.1262.

Livne S, Weiss D. 2014. Cytosolic activity of the gibberellin receptor GIBBERELLIN INSENSITIVE DWARF1A. *Plant & Cell Physiology* **55**:1727–1733 DOI 10.1093/pcp/pcu104.

Love MI, Huber W, Anders S. 2014. Moderated estimation of fold change and dispersion for RNA-seq data with DESeq2. *Genome Biology* **15**:550 DOI 10.1186/s13059-014-0550-8.

Luo H, Guo J, Ren X, Chen W, Huang L, Zhou X, Chen Y, Liu N, Xiong F, Lei Y, Liao B, Jiang H. 2018. Chromosomes A07 and A05 associated with stable and major QTLs for pod weight and size in cultivated peanut (*Arachis hypogaea* L.). *Theoretical & Applied Genetics* **131**:267–282 DOI 10.1007/s00122-017-3000-7.

Luo H, Ren X, Li Z, Xu Z, Li X, Huang L, Zhou X, Chen Y, Chen W, Lei Y, Liao B, Pandey MK, Varshney RK, Guo B, Jiang X, Liu F, Jiang H. 2017. Co-localization of major quantitative trait loci for pod size and weight to a 3.7 cM interval on chromosome A05 in cultivated peanut (*Arachis hypogaea* L.). *BMC Genomics* **18**:58 DOI 10.1186/s12864-016-3456-x.

Ma M, Wang Q, Li Z, Cheng H, Li Z, Liu X, Song W, Appels R, Zhao H. 2015. Expression of *TaCYP78A3*, a gene encoding cytochrome P450 CYP78A3 protein in wheat (*Triticum aestivum* L.), affects seed size. *The Plant Journal* **83**:312–325 DOI 10.1111/tpj.12896.

McAdam EL, Meitzel T, Quittenden LJ, Davidson SE, Dalmais M, Bendahmane AI, Thompson R, Smith JJ, Nichols DS, Urquhart S, Gélinas-Marion A, Aubert G, Ross JJ. 2017. Evidence that auxin is required for normal seed size and starch synthesis in pea. *New Phytologist* **216**:193–204 DOI 10.1111/nph.14690.

Moctezuma E. 1999. Changes in auxin patterns in developing gynophores of the peanut plant (*Arachis hypogaea* L.). *Annals of Botany* **83**:235–242 DOI 10.1006/anbo.1998.0814.

Moctezuma E. 2003. The peanut gynophore: a developmental and physiological perspective. *Canadian Journal of Botany* **81**:183–190 DOI 10.1139/b03-024.

Moctezuma E, Feldman LJ. 1998. Growth rates and auxin effects in graviresponding gynophores of the peanut, *Arachis hypogaea* (Fabaceae). *American Journal of Botany* **85**:1369–1376 DOI 10.2307/2446395.

Moctezuma E, Feldman LJ. 1999. Auxin redistributes upwards in graviresponding gynophores of the peanut plant. *Planta* **209**:180–186 DOI 10.1007/s004250050620.

Ogawa-Ohnishi M, Matsubayashi Y. 2015. Identification of three potent hydroxyproline O-galactosyltransferases in Arabidopsis. *Plant Journal* **81**:736–746 DOI 10.1111/tpj.12764.

Ohnishi T, Szatmari AM, Watanabe B, Fujita S, Bancos S, Koncz C, Lafos M, Shibata K, Yokota T, Sakata K, Szekeres M, Mizutani M. 2006. C-23 hydroxylation by Arabidopsis CYP90C1 and CYP90D1 reveals a novel shortcut in brassinosteroid biosynthesis. *Plant Cell* **18**:3275–3288 DOI 10.1105/tpc.106.045443.

Pertea M, Pertea GM, Antonescu CM, Chang TC, Mendell JT, Salzberg SL. 2015. StringTie enables improved reconstruction of a transcriptome from RNA-seq reads. *Nature Biotechnology* **33**:290–295 DOI 10.1038/nbt.3122.

Planas-Riverola A, Gupta A, Betegón-Putze I, Bosch N, Ibañes M, Caño Delgado AI. 2019. Brassinosteroid signaling in plant development and adaptation to stress. *Development* **146**:dev151894 DOI 10.1242/dev.151894.

Prigge MJ, Platre M, Kadakia N, Zhang Y, Greenham K, Szutu W, Pandey BK, Bhosale RA, Bennett MJ, Busch W, Estelle M. 2020. Genetic analysis of the Arabidopsis TIR1/AFB auxin receptors reveals both overlapping and specialized functions. *eLife* **9**:e54740 DOI 10.7554/eLife.54740.

Rieu I, Ruiz-Rivero O, Fernandez-Garcia N, Griffiths J, Powers SJ, Gong F, Linhartova T, Eriksson S, Nilsson O, Thomas SG, Phillips AL, Hedden P. 2008. The gibberellin biosynthetic genes *AtGA20ox1* and *AtGA20ox2* act, partially redundantly, to promote growth and development throughout the Arabidopsis life cycle. *Plant Journal* **53**:488–504 DOI 10.1111/j.1365-313X.2007.03356.x.

Saini S, Sharma I, Pati PK. 2015. Versatile roles of brassinosteroid in plants in the context of its homoeostasis, signaling and crosstalks. *Frontiers in Plant Science* **6**:950 DOI 10.3389/fpls.2015.00950.

Sampedro J, Gianzo C, Iglesias N, Guitián E, Revilla G, Zarra I. 2012. AtBGAL10 is the main xyloglucan β-galactosidase in Arabidopsis, and its absence results in unusual xyloglucan subunits and growth defects. *Plant Physiology* **158**:1146–1157 DOI 10.1104/pp.111.192195.

Schaller H. 2004. New aspects of sterol biosynthesis in growth and development of higher plants. *Plant Physiology & Biochemistry* **42**:465–476 DOI 10.1016/j.plaphy.2004.05.012.

Schrick K, Mayer U, Horrichs A, Kuhnt C, Bellini C, Dangl J, Schmidt J, Jürgens G. 2000. FACKEL is a sterol C-14 reductase required for organized cell division and expansion in Arabidopsis embryogenesis. *Genes & Development* **14**:1471–1484 DOI 10.1101/gad.14.12.1471.

Shannon P, Markiel A, Ozier O, Baliga NS, Wang JT, Ramage D, Amin N, Schwikowski B, Ideker T. 2003. Cytoscape: a software environment for integrated models of biomolecular interaction networks. *Genome Research* **13**:2498–2504 DOI 10.1101/gr.1239303.

Shao A, Ma W, Zhao X, Hu M, He X, Teng W, Li H, Tong Y. 2017. The auxin biosynthetic *TRYPTOPHAN AMINOTRANSFERASE RELATED TaTAR2.1-3A* increases grain yield of wheat. *Plant Physiology* **174**:2274–2288 DOI 10.1104/pp.17.00094.

Shlamovitz N, Ziv M, Zamski E. 1995. Light, dark and growth regulator involvement in groundnut (*Arachis hypogaea* L.) pod development. *Plant Growth Regulation* **16**:37–42 DOI 10.1007/BF00040505.

Shushu DD, Cutter EG. 1990. Growth of the gynophore of the peanut *Arachis hypogaea*. 2. Regulation of growth. *Canadian Journal of Botany* **68**:965–978 DOI 10.1139/b90-123.

Si J, Sun Y, Wang LU, Qin Y, Wang C, Wang X. 2016. Functional analyses of Populus euphratica brassinosteroid biosynthesis enzyme genes *DWF4* (*PeDWF4*) and *CPD* (*PeCPD*) in the regulation of growth and development of *Arabidopsis thaliana*. *Journal of Bioences* **41**:727–742 DOI 10.1007/s12038-016-9635-8.

Sinha P, Bajaj P, Pazhamala LT, Nayak SN, Pandey MK, Chitikineni A, Huai D, Khan AW, Desai A, Jiang H, Zhuang W, Guo B, Liao B, Varshney RK. 2020. Arachis hypogaea gene expression atlas for fastigiata subspecies of cultivated groundnut to accelerate functional and translational genomics applications. *Plant Biotechnology Journal* **18**:2187–2200 DOI 10.1111/pbi.13374.

Smith B. 1950. Arachis hypogaea. Aerial Flower and Subterranean Fruit. *American Journal of Botany* **37**:802–815 DOI 10.1002/j.1537-2197.1950.tb11073.x.

Stepanova AN, Robertson-Hoyt J, Yun J, Benavente LM, Xie DY, Dolezal K, Schlereth A, Jurgens G, Alonso JM. 2008. TAA1-mediated auxin biosynthesis is essential for hormone crosstalk and plant development. *Cell* **133**:177–191 DOI 10.1016/j.cell.2008.01.047.

Sun F, Ding L, Feng W, Cao Y, Lu F, Yang Q, Li W, Lu Y, Shabek N, Fu F, Yu H. 2021. Maize transcription factor ZmBES1/BZR1-5 positively regulates kernel size. *Journal of Experimental Botany* **72**:1714–1726 DOI 10.1093/jxb/eraa544.

Suzuki M, Kamide Y, Nagata N, Seki H, Ohyama K, Kato H, Masuda K, Sato S, Kato T, Tabata S, Yoshida S, Muranaka T. 2004. Loss of function of *3-hydroxy-3-methylglutaryl coenzyme A reductase 1* (*HMG1*) in Arabidopsis leads to dwarfing, early senescence and male sterility, and reduced sterol levels. *Plant Journal* **37**:750–761 DOI 10.1111/j.1365-313x.2004.02003.x.

Tong H, Xiao Y, Liu D, Gao S, Liu L, Yin Y, Jin Y, Qian Q, Chu C. 2014. Brassinosteroid regulates cell elongation by modulating gibberellin metabolism in rice. *Plant Cell* **26**:4376–4393 DOI 10.1105/tpc.114.132092.

Unterholzner SJ, Rozhon W, Papacek M, Ciomas J, Lange T, Kugler KG, Mayer KF, Sieberer T, Poppenberger B. 2015. Brassinosteroids are master regulators of gibberellin biosynthesis in Arabidopsis. *Plant Cell* **27**:2261–2272 DOI 10.1105/tpc.15.00433.

Vanstraelen M, Benková E. 2012. Hormonal interactions in the regulation of plant development. *Annual Review of Cell and Developmental Biology* **28**:463–487 DOI 10.1146/annurev-cellbio-101011-155741.

Wan LY, Li B, Lei Y, Yan LY, Ren XP, Chen YN, Dai XF, Jiang HF, Zhang JC, Guo W, Chen A, Liao BS. 2017. Mutant transcriptome sequencing provides insights into pod development in peanut (*Arachis hypogaea* L.). *Frontiers in Plant Science* **8**:1900 DOI 10.3389/fpls.2017.01900.

Wang Y, Li B, Du M, Eneji AE, Wang B, Duan L, Li Z, Tian X. 2012. Mechanism of phytohormone involvement in feedback regulation of cotton leaf senescence induced by potassium deficiency. *Journal of Experimental Botany* **63**:5887–5901 DOI 10.1093/jxb/ers238.

Wang B, Sang Y, Song J, Gao X, Zhang X. 2009. Expression of a rice *OsARGOS* gene in Arabidopsis promotes cell division and expansion and increases organ size. *Journal of Genetics and Genomics* **36**:31–40 DOI 10.1016/S1673-8527(09)60004-7.

Wang J, Tang M, Chen S, Zheng X, Mo H, Li S, Wang Z, Zhu K, Ding L, Liu S, Li Y, Tan X. 2017. Down-regulation of BnDA1, whose gene locus is associated with the seeds weight, improves the seeds weight and organ size in *Brassica napus*. *Plant Biotechnology Journal* **8**:1024–1033.

Wang J, Wang R, Mao X, Zhang J, Liu Y, Xie Q, Yang X, Chang X, Li C, Zhang X, Jing R. 2020. RING finger ubiquitin E3 ligase gene *TaSDIR1-4A* contributes to determination of grain size in common wheat. *Journal of Experimental Botany* **71**:5377–5388 DOI 10.1093/jxb/eraa271.

Xia H, Zhao C, Hou L, Li A, Zhao S, Bi Y, An J, Zhao Y, Wan S, Wang X. 2013. Transcriptome profiling of peanut gynophores revealed global reprogramming of gene expression during early pod development in darkness. *BMC Genomics* **14**:517 DOI 10.1186/1471-2164-14-517.

Xu J, Li J, Cui L, Zhang T, Wu Z, Zhu P, Meng Y, Zhang K, Yu X, Lou Q, Chen J. 2017. New insights into the roles of cucumber TIR1 homologs and miR393 in regulating fruit/seed set development and leaf morphogenesis. *BMC Plant Biology* **17**:130 DOI 10.1186/s12870-017-1075-6.

Yamaguchi K, Yamamoto T, Segami S, Horikawa M, Chaya G, Kitano H, Iwasaki Y, Miura K. 2020. gw2 mutation increases grain width and culm thickness in rice (*Oryza sativa* L.). *Breeding Science* **70**:456–461 DOI 10.1270/jsbbs.20018.

Yang S, Wang J, Tang Z, Guo F, Zhang Y, Zhang J, Meng J, Zheng L, Wan S, Li X. 2020. Transcriptome of peanut kernel and shell reveals the mechanism of calcium on peanut pod development. *Scientific Reports* **10**:15723 DOI 10.1038/s41598-020-72893-9.

Yin D, Wang Y, Zhang X, Li H, Lu X, Zhang J, Zhang W, Chen S. 2013. De novo assembly of the peanut (*Arachis hypogaea* L.) seed transcriptome revealed candidate unigenes for oil accumulation pathways. *PLOS ONE* **8**:e73767 DOI 10.1371/journal.pone.0073767.

Zhang X, Guo W, Du D, Pu L, Zhang C. 2020. Overexpression of a maize BR transcription factor ZmBZR1 in Arabidopsis enlarges organ and seed size of the transgenic plants. *Plant Science* **292**:110378 DOI 10.1016/j.plantsci.2019.110378.

Zhang Y, Wang P, Xia H, Zhao C, Hou L, Li C, Gao C, Wang X, Zhao S. 2016. Comparativetranscriptome analysis of basal and zygote-located tip regions of peanut ovaries provides insight into the mechanism of light regulation in peanut embryo and pod development. *BMC Genomics* **17**:606 DOI 10.1186/s12864-016-2857-1.

Zhuang WJ, Chen H, Yang M, Wang JP, Pandey MK, Zhang C, Chang WC, Zhang LS, Zhang XT, Tang RH, Garg V, Wang XJ, Tang HB, Chow CN, Wang JP, Deng Y, Wang DP, Khan AW, Yang Q, Cai TC, Bajaj P, Wu KC, Guo BZ, Zhang XY, Li JJ, Liang F, Hu J, Liao BS, Liu SY, Chitikineni A, Yan HS, Zheng YX, Shan SH, Liu QZ, Xie DY, Wang ZY, Khan SZ, Ali N, Zhao CZ, Li XG, Luo ZL, Zhang SB, Zhuang RR, Peng Z, Wang SY, Mamadou G, Zhuang YH, Zhao ZF, Yu WC, Xiong FQ, Quan WP, Yuan M, Li Y, Zou HS, Xia H, Zha L, Fan JP, Yu JG, Xie WP, Yuan JQ, Chen K, Zhao SS, Chu WT, Chen YT, Sun PC, Meng FB, Zhuo T, Zhao YH, Li CJ, He GH, Zhao YL, Wang CC, Kavikishor PB, Pan RL, Paterson AH, Wang XY, Ming R, Varshney RK. 2019. The genome of cultivated peanut provides insight into legume karyotypes, polyploid evolution and crop domestication. *Nature Genetics* **51**:865–876 DOI 10.1038/s41588-019-0402-2.